

Supplemental information

**Combined tumor and immune signals
from genomes or transcriptomes predict
outcomes of checkpoint inhibition in melanoma**

Samuel S. Freeman, Moshe Sade-Feldman, Jaegil Kim, Chip Stewart, Anna L.K. Gonye, Arvind Ravi, Monica B. Arniella, Irena Gushterova, Thomas J. LaSalle, Emily M. Blaum, Keren Yizhak, Dennie T. Frederick, Tatyana Sharova, Ignaty Leshchiner, Liudmila Elagina, Oliver G. Spiro, Dimitri Livitz, Daniel Rosebrock, François Aguet, Jian Carrot-Zhang, Gavin Ha, Ziao Lin, Jonathan H. Chen, Michal Barzily-Rokni, Marc R. Hammond, Hans C. Vitzthum von Eckstaedt, Shauna M. Blackmon, Yunxin J. Jiao, Stacey Gabriel, Donald P. Lawrence, Lyn M. Duncan, Anat O. Stemmer-Rachamimov, Jennifer A. Wargo, Keith T. Flaherty, Ryan J. Sullivan, Genevieve M. Boland, Matthew Meyerson, Gad Getz, and Nir Hacohen

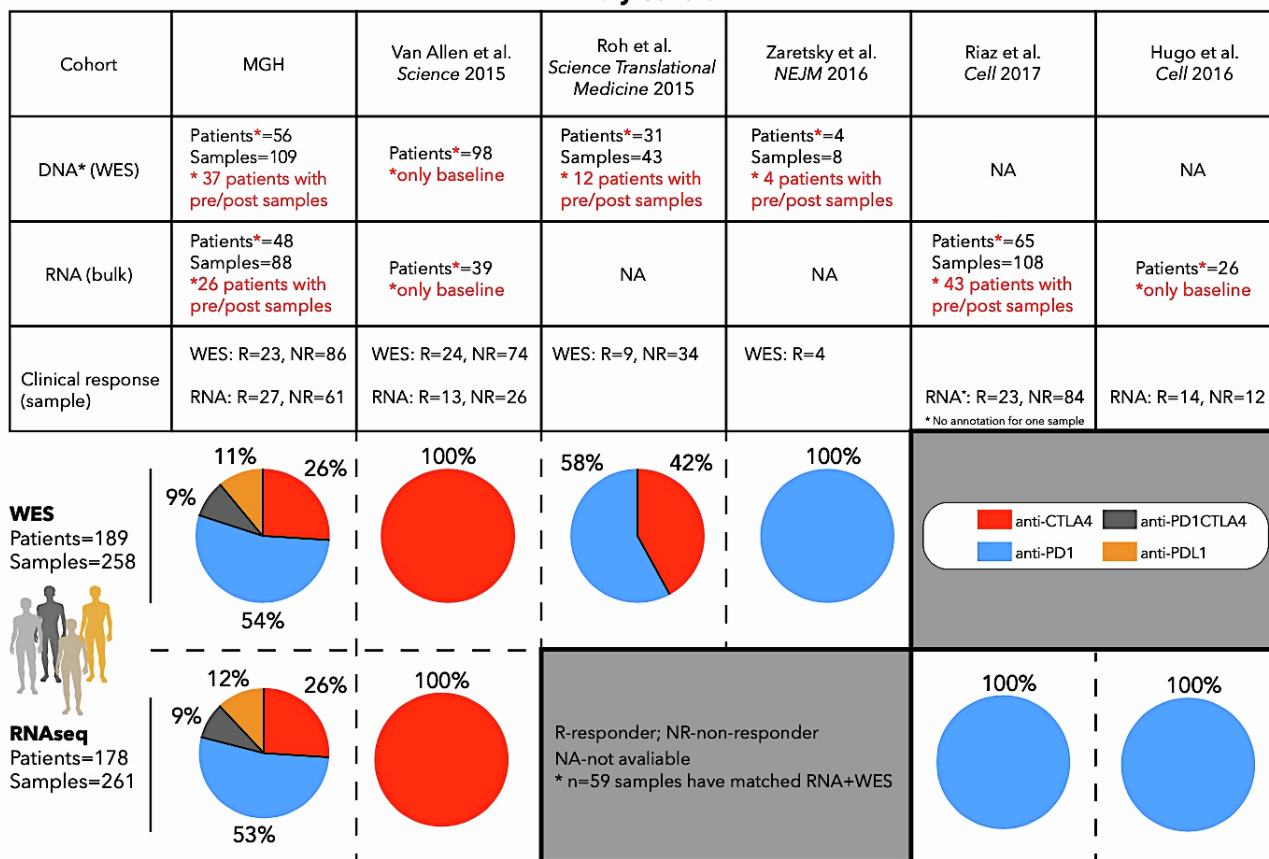
Supplementary Figures

List of Supplementary Figures:

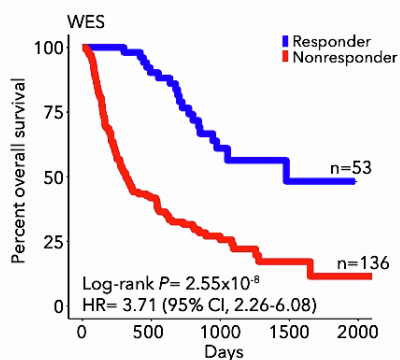
- Supplementary Figure 1: Primary cohort composition in meta-analysis and analysis workflow, Related to Figure 1 and STAR methods quantification and statistical analysis
- Supplementary Figure 2: TMB, neoantigens, tumor purity and single gene mutation models, Related to Figure 1
- Supplementary Figure 3: Comparison between paired pre-treatment and post-treatment biopsies, Related to Figure 1
- Supplementary Figure 4: Performance of TCB_{RNA} and BCB_{RNA} models, Related to Figure 2
- Supplementary Figure 5: Performance of TCB_{DNA} and BCB_{DNA} models, Related to Figure 2
- Supplementary Figure 6: Performance of integrative DNA-based models for survival and response prediction, Related to Figure 2
- Supplementary Figure 7: Quantification of immune and stromal cell fractions using CIBERSORTx, Related to Figure 2
- Supplementary Figure 8: Performance of integrative DNA-based models for survival and response prediction for TCGA melanoma stage III-IV cases, Related to Figure 2
- Supplementary Figure 9: Dynamics of DNA and RNA-based TCB and BCB abundance between paired pre-treatment and post-treatment biopsies, Related to Figure 2
- Supplementary Figure 10: Subtypes identified using NMF clustering of TCGA melanoma RNA-seq and their tumor related features, Related to Figure 3
- Supplementary Figure 11: Subtype classification for pre-immunotherapy RNA-seq samples, Related to Figure 3
- Supplementary Figure 12: Genes associated with response in the primary cohort and expression patterns for long and short OS differentially expressed genes in the primary cohort, Related to Figure 3
- Supplementary Figure 13: Expression patterns for responder and non-responder differentially expressed genes and performance of gene-pair models in the primary cohort, Related to Figure 3 and Figure 4
- Supplementary Figure 14: Performance of the three RNA gene-pair models with TMB in the primary cohort, expression of genes from top gene pair models and gene pair model performance, Related to Figure 4
- Supplementary Figure 15: Cross-validation of gene pair model discovery and validation in the primary cohort, Related to Figure 4
- Supplementary Figure 16: Batch effects correction and melanoma subtyping for the secondary cohort, Related to Figure 4
- Supplementary Figure 17: Performance of top gene pair models in the secondary cohort, Related to Figure 4
- Supplementary Figure 18: Performance of all models within each cohort separately, Related to Figure 4
- Supplementary Figure 19: Performance of all models in patients treated with different checkpoint blockade therapies, Related to Figure 4
- Supplementary Figure 20: Analysis of melanoma TBX3 expression, Related to Figure 4

A

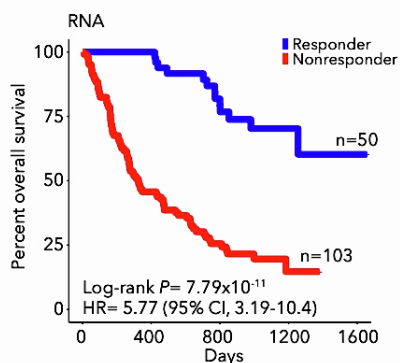
Primary Cohort



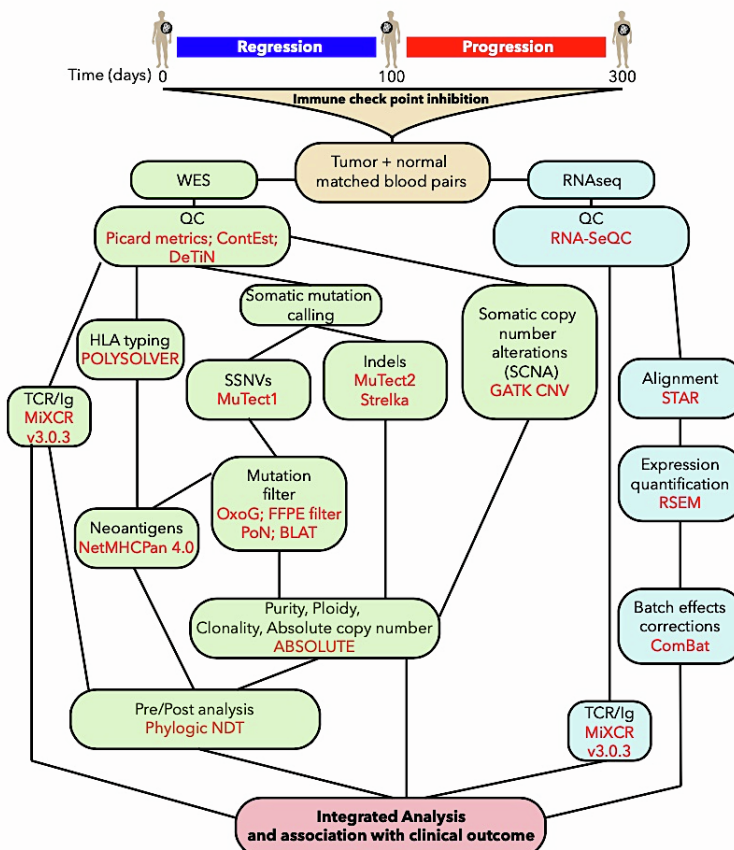
B



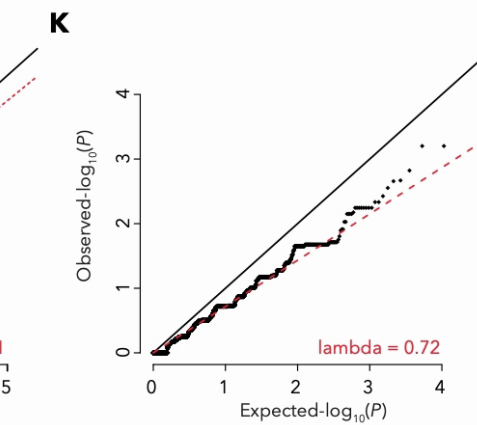
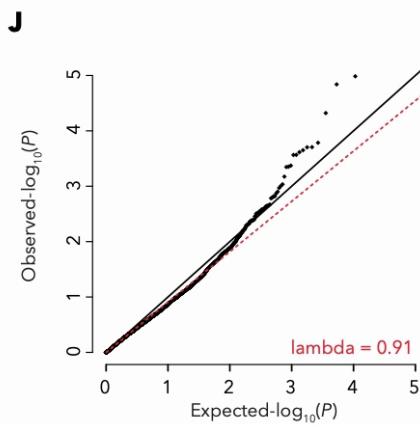
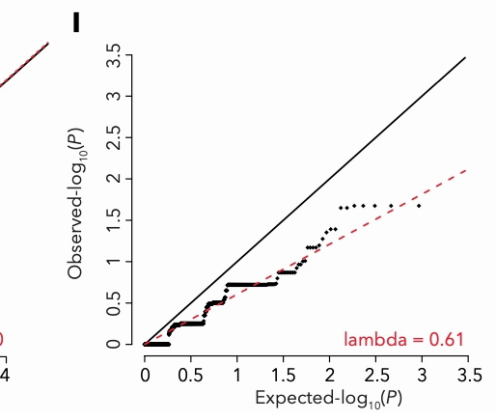
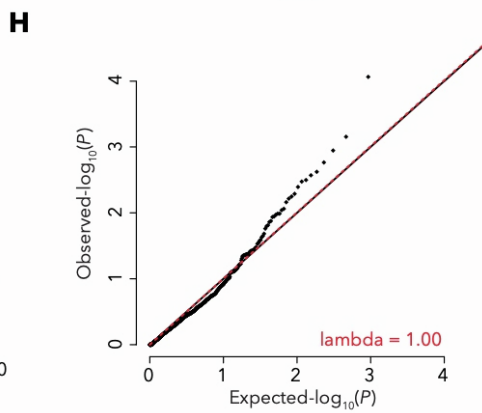
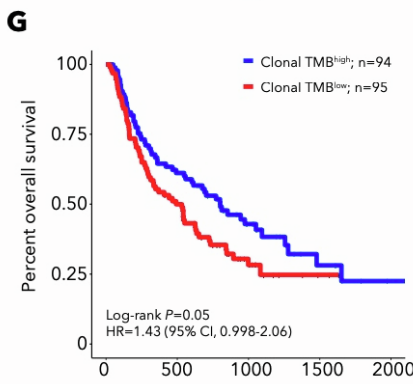
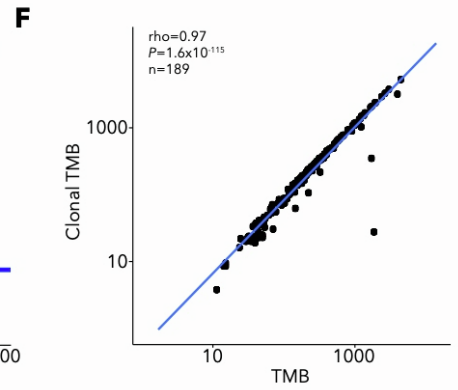
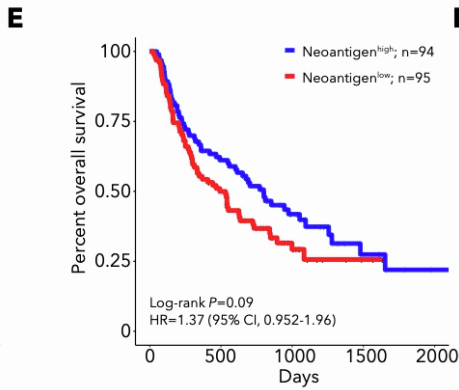
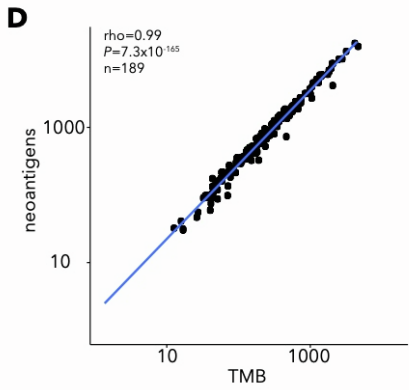
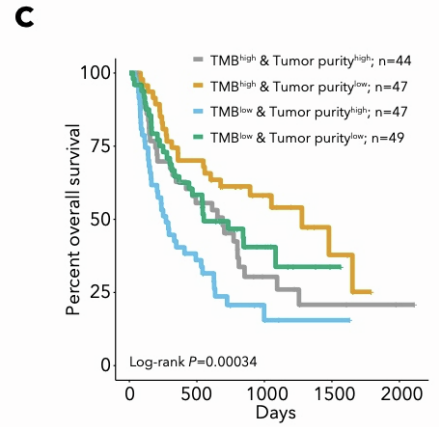
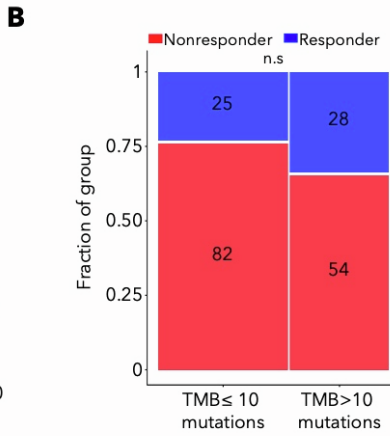
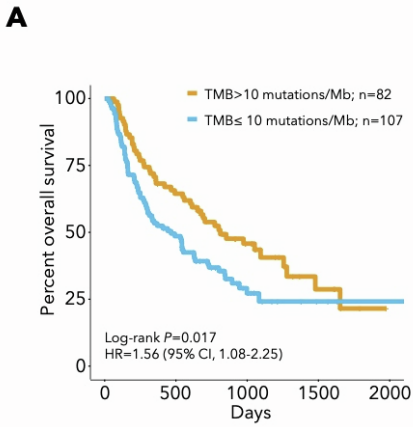
C



D

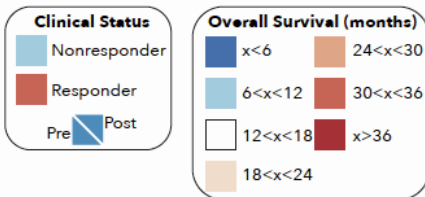
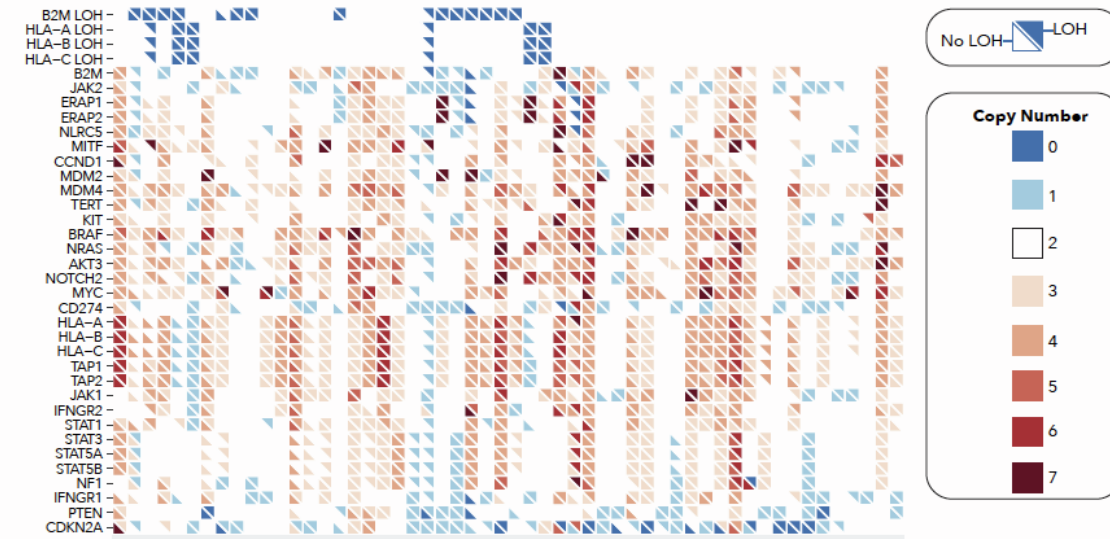
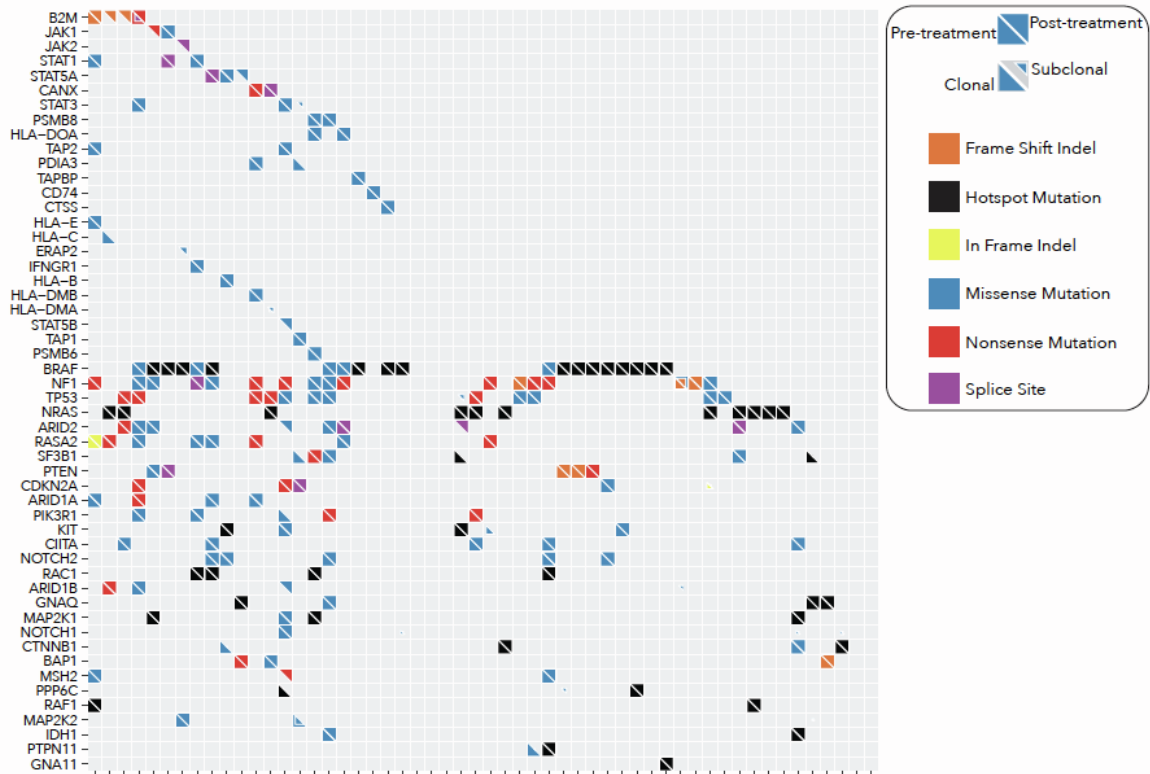


Supplementary Figure 1. Primary cohort composition in meta-analysis and analysis workflow, Related to Figure 1 and STAR methods quantification and statistical analysis. **A.** Six cohorts were included in the primary cohort meta-analysis. Table indicated cohorts for which DNA and/or RNA was available. The clinical response and numbers of pre-treatment and post-treatment samples are indicated for each cohort. Treatment for patients in each cohort is indicated in the pie charts. **B-C.** Kaplan-Meier survival curve for responders and nonresponders in the primary cohort for DNA (WES) (**B**) and RNA (**C**) samples is shown. One patient in the Hugo cohort had response data but no survival data. **D.** Flow chart of analysis pipeline used to process DNA (WES) and RNA-seq data in this study.

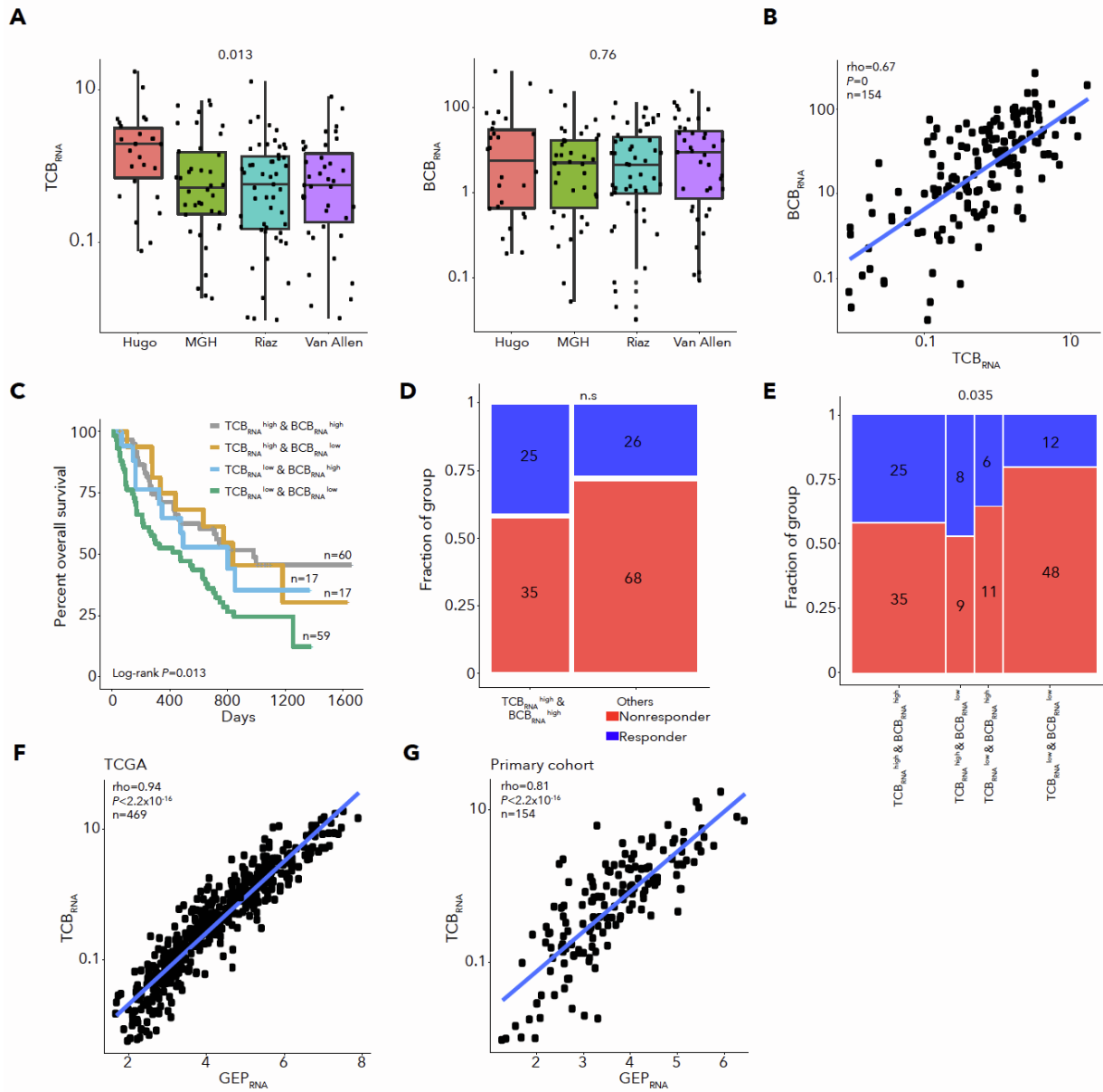


Supplementary Figure 2. TMB, neoantigens, tumor purity and single gene mutation models, Related to Figure 1.

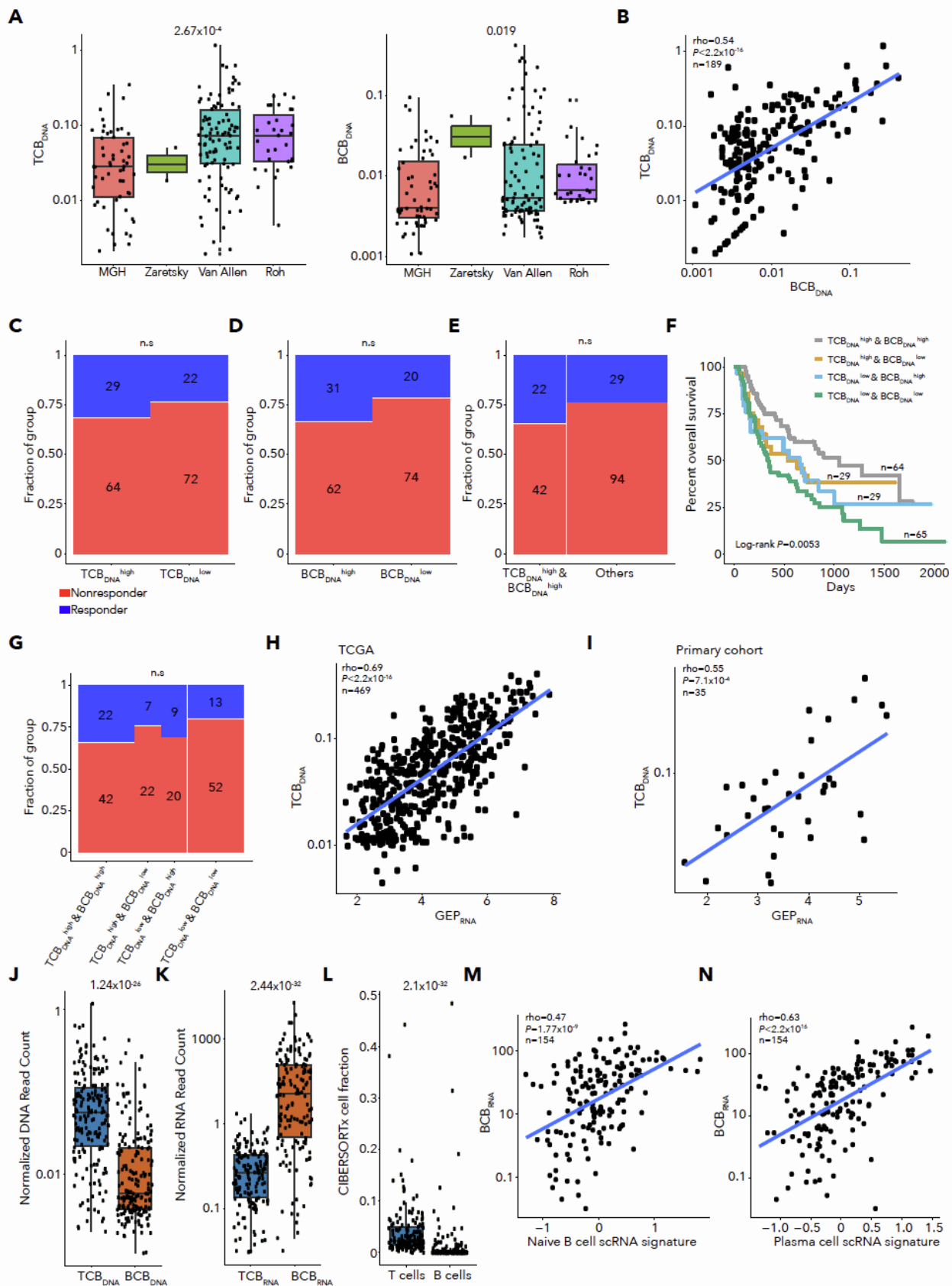
A. Kaplan-Meier survival curve for TMB high and low subgroups using TMB=10 mutations/Mb as a threshold (rather than the median). **B.** Response for patients with TMB over or under 10 mutations/Mb. **C.** Kaplan-Meier survival curve for all four subgroups of TMB (using the median threshold) and tumor purity. **D.** Spearman correlation of TMB with the number of neoantigens. **E.** Kaplan-Meier survival curve for patients with neoantigen burden above or below median. **F.** Correlation between clonal non-silent mutation burden (Clonal TMB) and TMB. **G.** Kaplan-Meier survival curve for patients with clonal TMB above or below median. **H.** qq plot for p values of the addition of each gene's mutation status to TMB in a Cox model for survival using loss-of-function mutation status for genes with 3 or more loss-of-function mutations. **I.** qq plot for p values of the addition of each gene's mutation status to TMB in a logistic regression model for response status using loss-of-function mutation status for genes with 3 or more loss-of-function mutations. **J.** qq plot for p values of the addition of each gene's mutation status to TMB in a Cox model for survival using non-synonymous mutation status for genes with 3 or more non-synonymous mutations. **K.** qq plot for p values of the addition of each gene's mutation status to TMB in a logistic regression model for response status using non-synonymous mutation status for genes with 3 or more non-synonymous mutations.



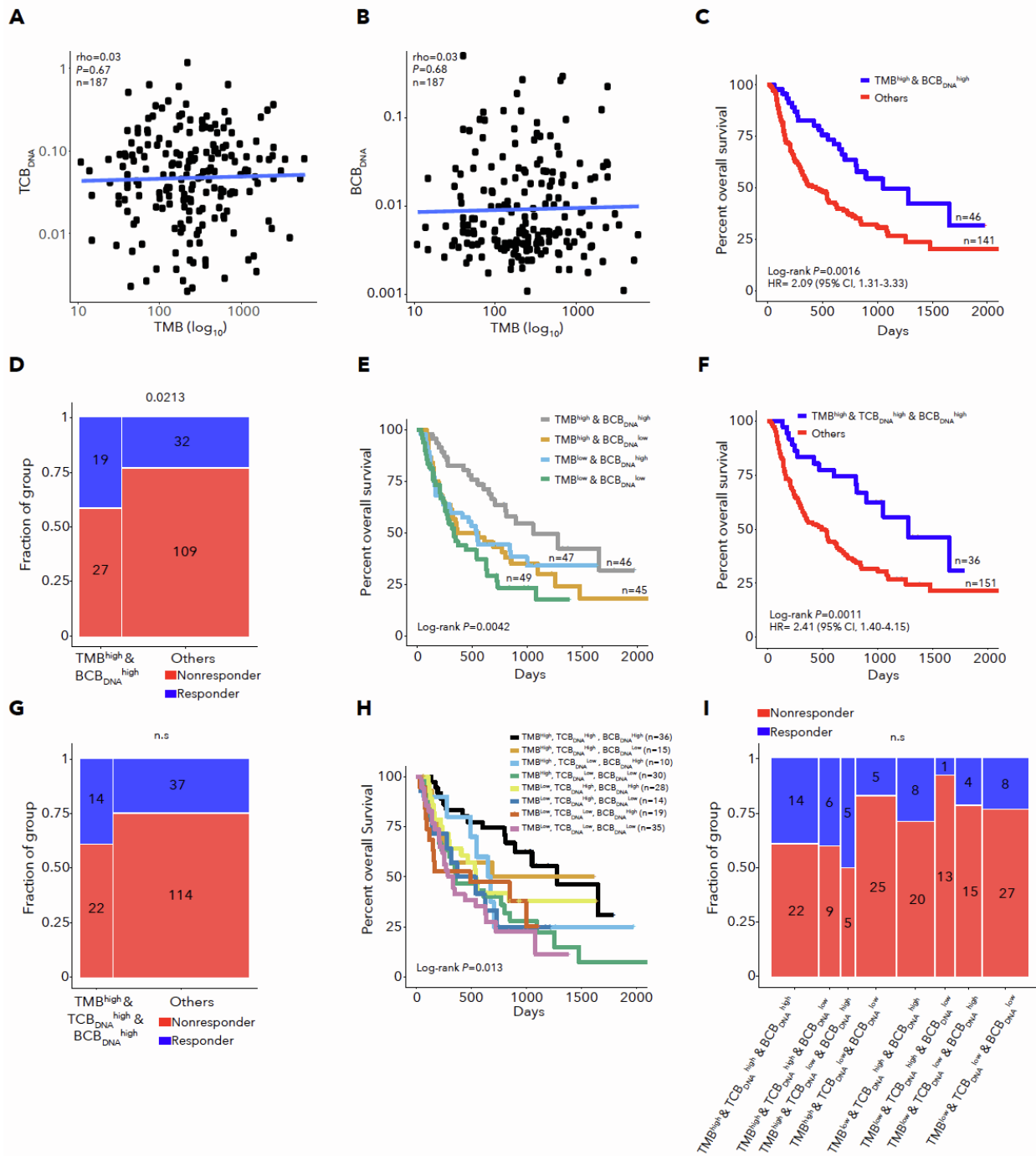
Supplementary Figure 3. Comparison between paired pre-treatment and post-treatment biopsies, Related to Figure 1. Upper panel shows a plot of mutations for selected genes in matched pre-treatments and post-treatment biopsies. The lower panel shows the integer copy number and LOH status for selected genes. Mutation clonality is represented by the area of each triangle in the upper panel. Lower triangles indicate mutations or copy number pre-treatment and upper triangles indicate mutations or copy number post-treatment. In the lower panel, white indicates absence of LOH in the first four rows and a copy number of 2 in the remaining rows. Patient response characteristics and survival are shown in the bottom two rows.



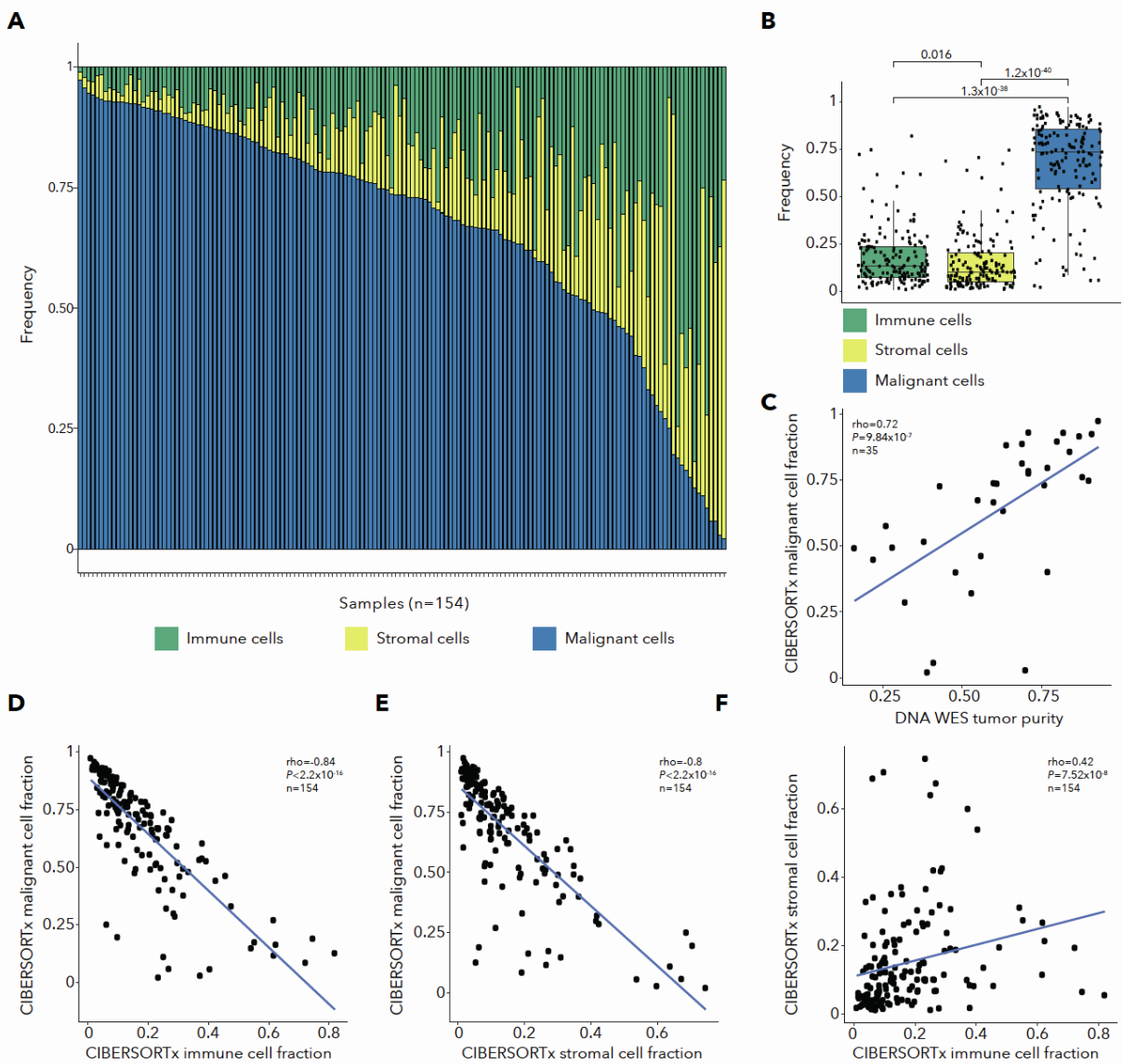
Supplementary Figure 4. Performance of TCB_{RNA} and BCB_{RNA} models, Related to Figure 2. **A.** TCB_{RNA} (left) and BCB_{RNA} (right) for each cohort with Kruskal-Wallis test p values. **B.** Correlation between TCB_{RNA} and BCB_{RNA} for primary cohort samples. **C.** Kaplan-Meier survival curve for all TCB_{RNA} and BCB_{RNA} high and low subgroups. **D.** Response for TCB_{RNA} high, BCB_{RNA} high subgroup vs. others. **E.** Response for all TCB_{RNA} and BCB_{RNA} high and low subgroups. **F.** Correlation between TCB_{RNA} and GEP³² in TCGA melanoma samples. **G.** Correlation between TCB_{RNA} and GEP in primary cohort samples.



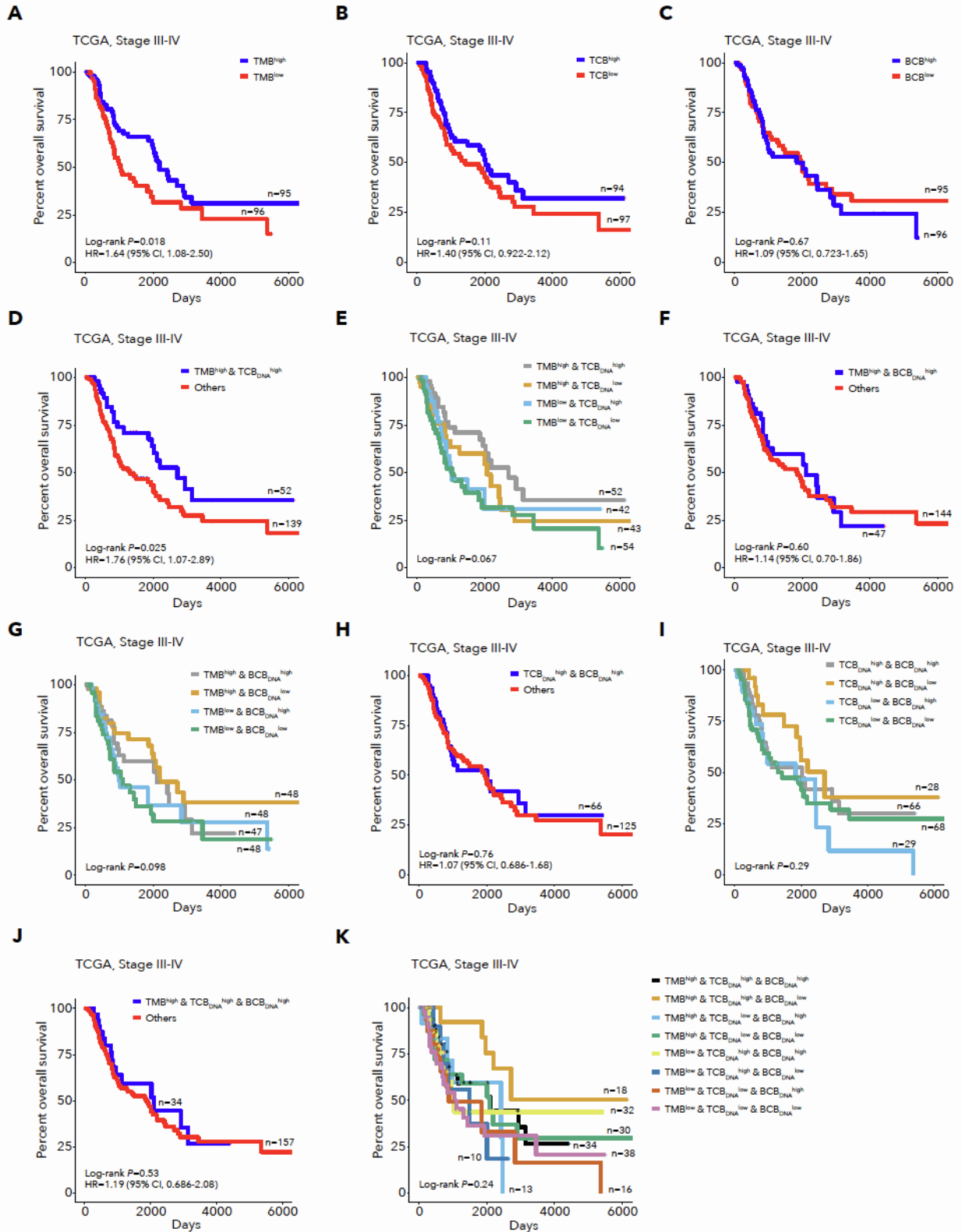
Supplementary Figure 5. Performance of TCB_{DNA} and BCB_{DNA} models, Related to Figure 2. **A.** TCB_{DNA} (left) and BCB_{DNA} (right) for each cohort with Kruskal-Wallis test p values. Due to cohort differences, we classified samples as above or below median TCB_{DNA} or BCB_{DNA} within each cohort. **B.** Correlation between TCB_{DNA} and BCB_{DNA} for primary cohort samples. **C.** Response for TCB_{DNA} high and low subgroups. **D.** Response for BCB_{DNA} high and low subgroups. **E.** Response for TCB_{DNA} high, BCB_{DNA} high subgroup vs. others. **F.** Kaplan-Meier survival curve for all TCB_{DNA} and BCB_{DNA} high and low subgroups. **G.** Response for all TCB_{DNA} and BCB_{DNA} high and low subgroups. **H.** Correlation between TCB_{DNA} and GEP_{RNA}³² in TCGA melanoma samples. **I.** Correlation between TCB_{DNA} and GEP_{RNA} in primary cohort samples, for samples with DNA and RNA extracted from the same location in the tumor. **J.** Normalized DNA read counts for TCB_{DNA} vs. BCB_{DNA} comparison, with Wilcoxon test p value. **K.** Normalized RNA read counts for TCB_{RNA} vs. BCB_{RNA} comparison, with Wilcoxon test p value. **L.** CIBERSORTx cell fraction for T cells and B cells, with Wilcoxon test p value. **M.** Correlation between BCB_{RNA} and naive B cell scRNA signature for primary cohort samples. **N.** Correlation between BCB_{RNA} and plasma B cell scRNA signature for primary cohort samples.



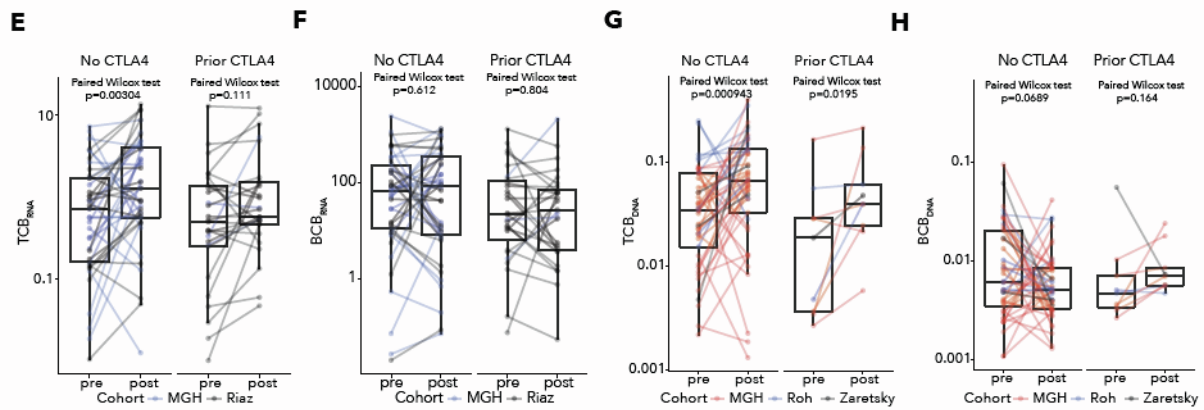
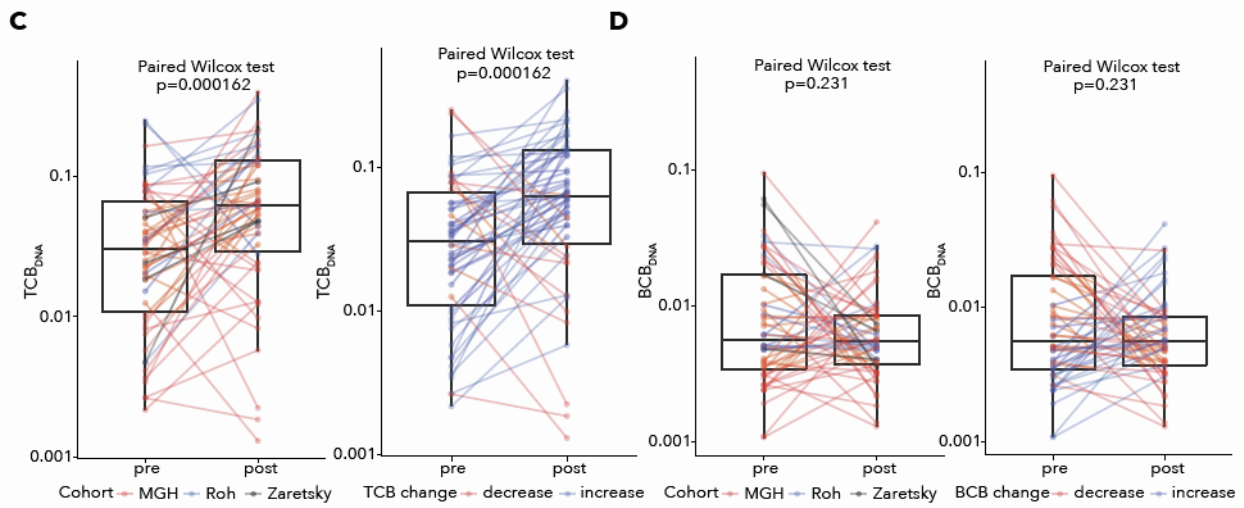
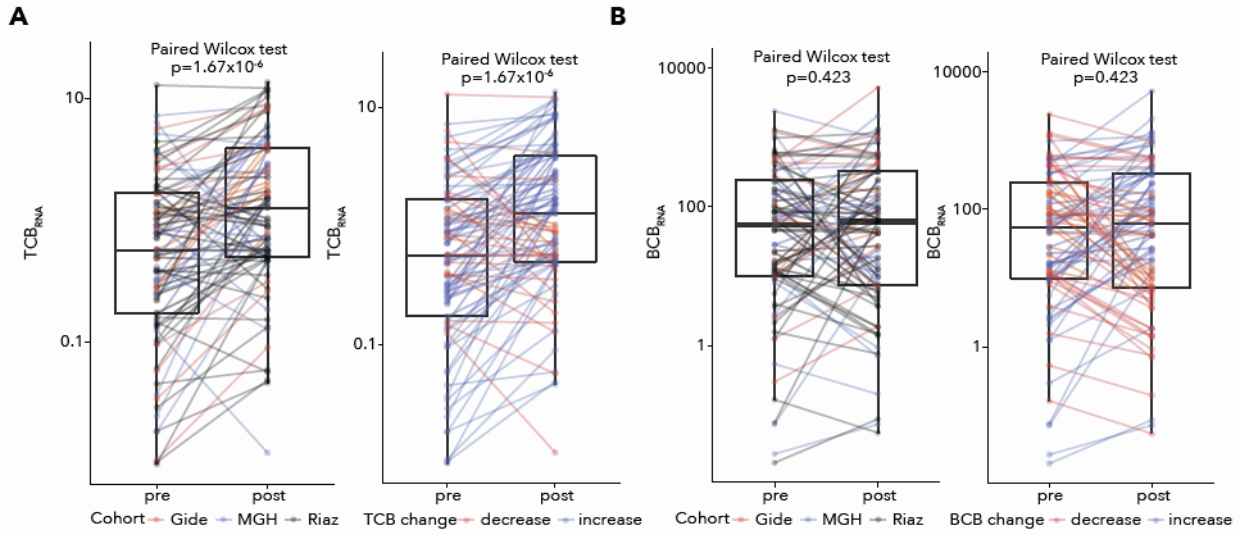
Supplementary Figure 6. Performance of integrative DNA-based models for survival and response prediction, Related to Figure 2. **A.** Correlation between TMB and TCB_{DNA} . **B.** Correlation between TMB and BCB_{DNA} . **C.** Kaplan-Meier survival curve for TMB high, BCB_{DNA} high subgroup vs. other patients. **D.** Response for TMB high, BCB_{DNA} high subgroup vs. other patients. **E.** Kaplan-Meier survival curve for all combined TMB and BCB_{DNA} subgroups. **F.** Kaplan-Meier survival curve for TMB high, TCB_{DNA} high, BCB_{DNA} high subgroup vs. other patients. **G.** Response for TMB high, TCB_{DNA} high, BCB_{DNA} high subgroup vs. other patients. **H.** Kaplan-Meier survival curve for all combined TMB , TCB_{DNA} , and BCB_{DNA} subgroups. **I.** Response for all combined TMB , TCB_{DNA} , and BCB_{DNA} subgroups.



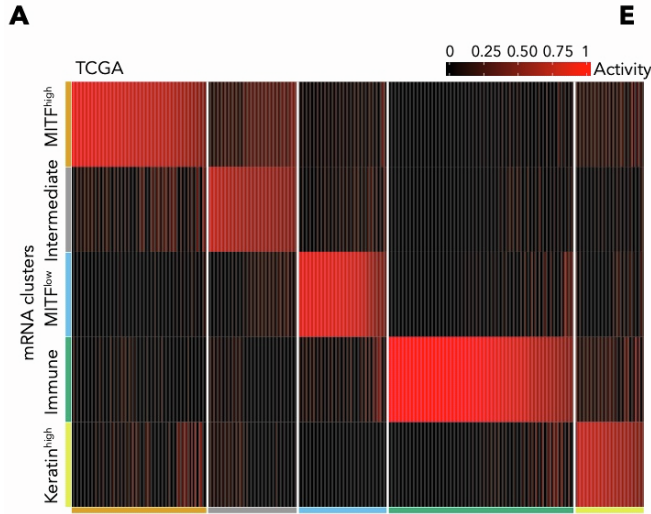
Supplementary Figure 7. Quantification of immune and stromal cell fractions using CIBERSORTx, Related to Figure 2. **A.** CIBERSORTx immune, stromal and malignant cell fractions for each patient in primary cohort RNA samples (n=154). **B.** Cell fraction estimation for immune, stromal and malignant cells using CIBERSORTx, with Wilcoxon test p value. **C.** Correlation between CIBERSORTx malignant cell fraction from RNA-Seq and DNA WES tumor purity for samples with matched DNA and RNA from the same tumor location in primary cohort (n=35). **D.** Correlation between CIBERSORTx immune and malignant cell fractions for primary cohort samples. **E.** Correlation between CIBERSORTx stromal and malignant cell fractions for primary cohort samples. **F.** Correlation between CIBERSORTx immune and stromal cell fractions for primary cohort samples.



Supplementary Figure 8. Performance of integrative DNA-based models for survival and response prediction for TCGA melanoma stage III-IV cases, Related to Figure 2. **A.** Kaplan-Meier survival curve for TMB high and low subgroups. **B.** Kaplan-Meier survival curve for TCB_{DNA} high vs. other patients. **C.** Kaplan-Meier survival curve for BCB_{DNA} high vs. other patients. **D.** Kaplan-Meier survival curve for TMB high, TCB_{DNA} high subgroup vs. other patients. **E.** Kaplan-Meier survival curve for all combined TMB and TCB_{DNA} subgroups. **F.** Kaplan-Meier survival curve for TMB high, BCB_{DNA} high subgroup vs. other patients. **G.** Kaplan-Meier survival curve for all combined TMB and BCB_{DNA} subgroups. **H.** Kaplan-Meier survival curve for TCB_{DNA} high, BCB_{DNA} high subgroup vs. other patients. **I.** Kaplan-Meier survival curve for all combined TCB_{DNA} and BCB_{DNA} subgroups. **J.** Kaplan-Meier survival curve for TMB high, TCB_{DNA} high, BCB_{DNA} high subgroup vs. other patients. **K.** Kaplan-Meier survival curve for all combined TMB, TCB_{DNA} and BCB_{DNA} subgroups.



Supplementary Figure 9. Dynamics of DNA and RNA-based TCB and BCB abundance between paired pre-treatment and post-treatment biopsies, Related to Figure 2. **A.** Changes in TCB_{RNA} between matched pre-treatment and post-treatment samples, colored by cohort (left) or decrease/increase (right). **B.** Changes in BCB_{RNA} between matched pre-treatment and post-treatment samples, colored by cohort (left) or decrease/increase (right). **C.** Changes in TCB_{DNA} between matched pre-treatment and post-treatment samples, colored by cohort (left) and decrease/increase (right). **D.** Changes in BCB_{DNA} between matched pre-treatment and post-treatment samples, colored by cohort (left) and decrease/increase (right). **E.** Changes in TCB_{RNA} between matched pre-treatment and post-treatment samples, with no prior CTLA-4 therapy (left) or prior CTLA-4 therapy (right). **F.** Changes in BCB_{RNA} between matched pre-treatment and post-treatment samples, with no prior CTLA-4 therapy (left) or prior CTLA-4 therapy (right). **G.** Changes in TCB_{DNA} between matched pre-treatment and post-treatment samples, with no prior CTLA-4 therapy (left) or prior CTLA-4 therapy (right). **H.** Changes in BCB_{DNA} between matched pre-treatment and post-treatment samples, with no prior CTLA-4 therapy (left) or prior CTLA-4 therapy (right).



B

	MITF ^{high}	Intermediate	MITF ^{low}	Immune	Keratin ^{high}
*Keratin	58	19	0	2	23
*MITF ^{low}	3	17	39	0	0
*Immune	16	12	16	115	9

*TCGA melanoma subtypes (Cell 2015)

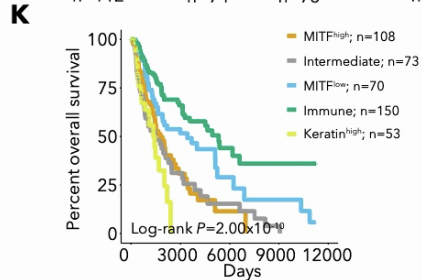
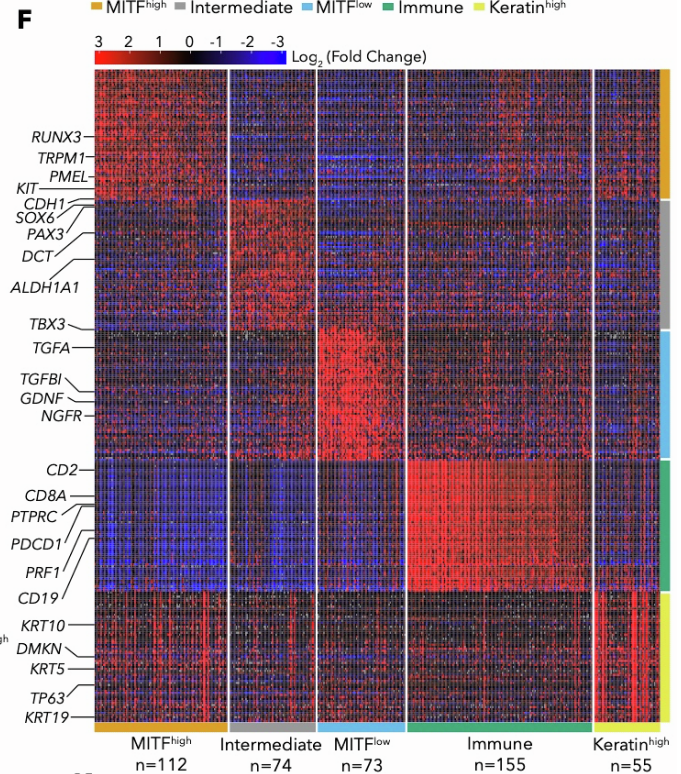
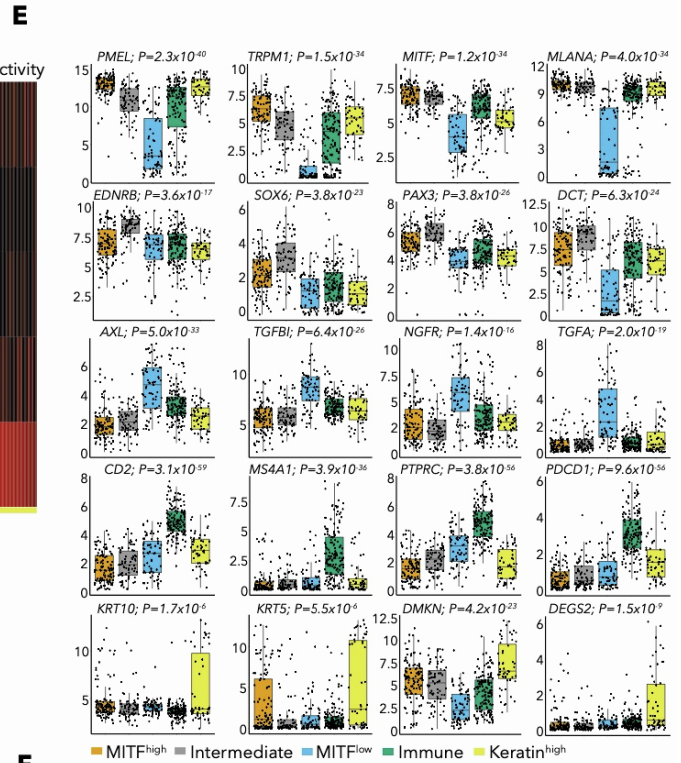
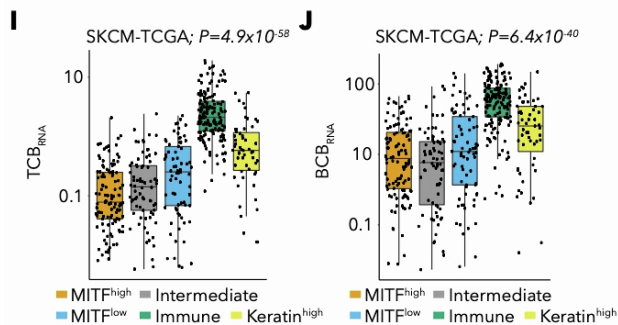
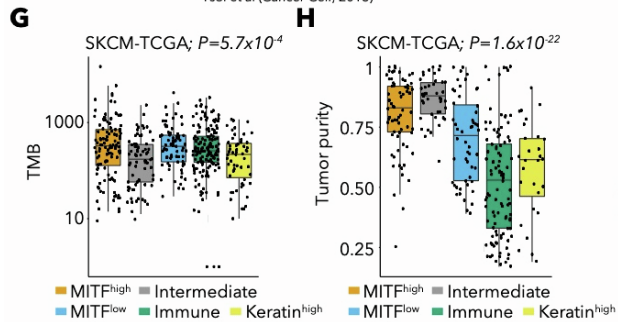
C

	MITF ^{high}	Intermediate	MITF ^{low}	Immune	Keratin ^{high}
Distant metastasis	23	13	13	13	6
Primary tumor	35	21	5	15	26
Cutaneous tissue	13	12	23	20	6
Lymph node	40	27	32	106	16

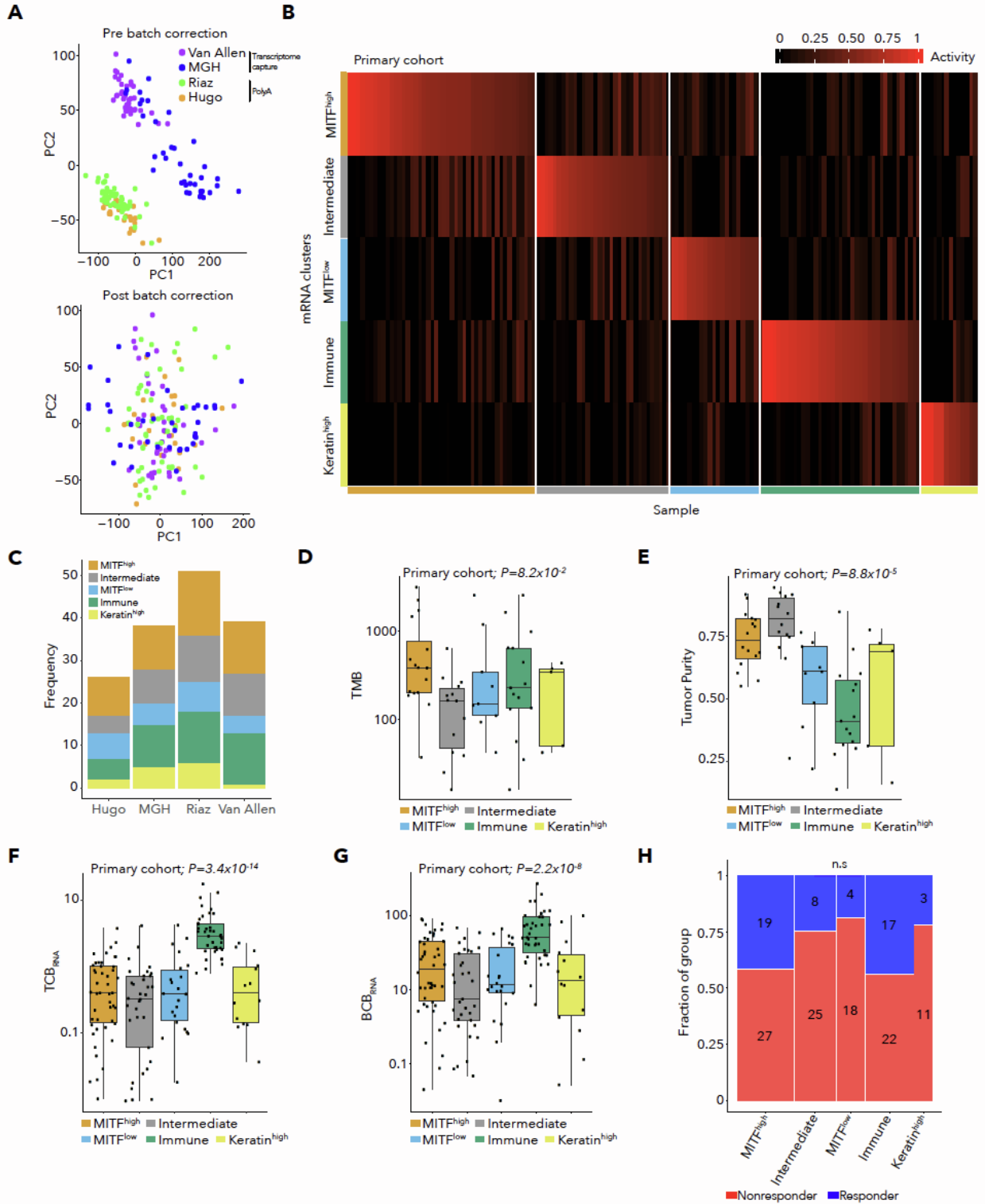
D

	MITF ^{high}	Intermediate	MITF ^{low}	Immune	Keratin ^{high}
Melanocytic	74	6	0	20	22
Transitory	38	68	34	121	31
Neural crest-like	0	0	29	8	0
Undifferentiated	0	0	10	5	1

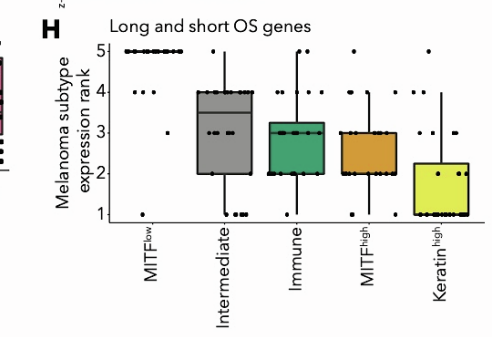
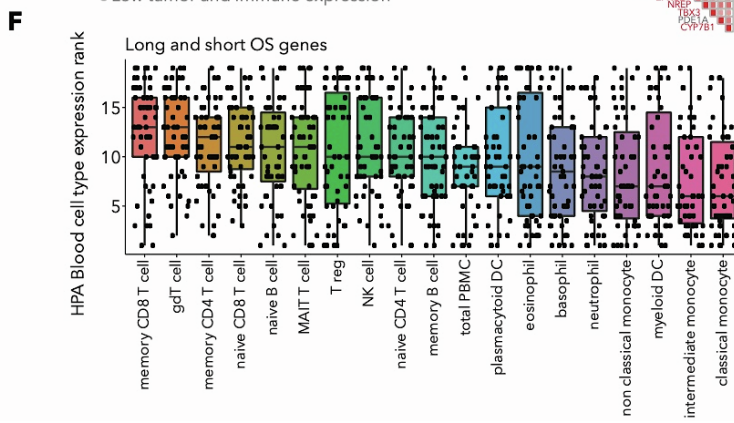
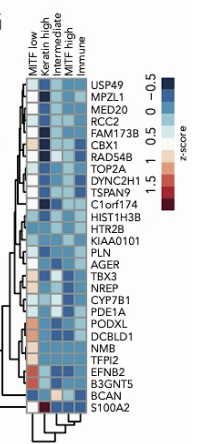
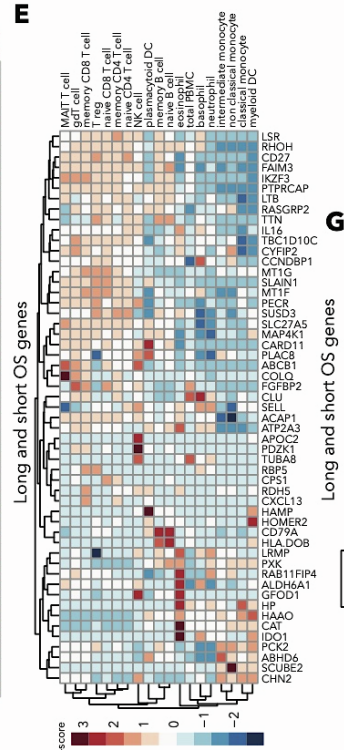
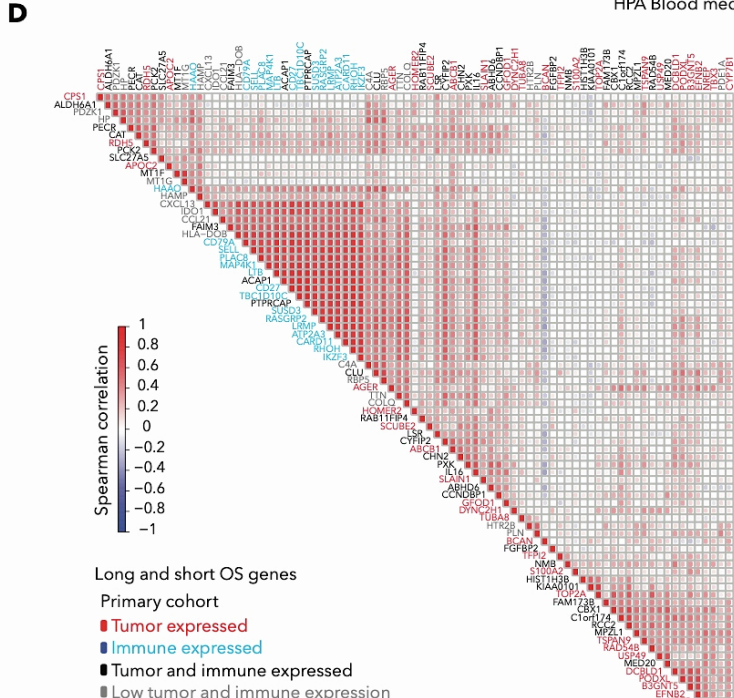
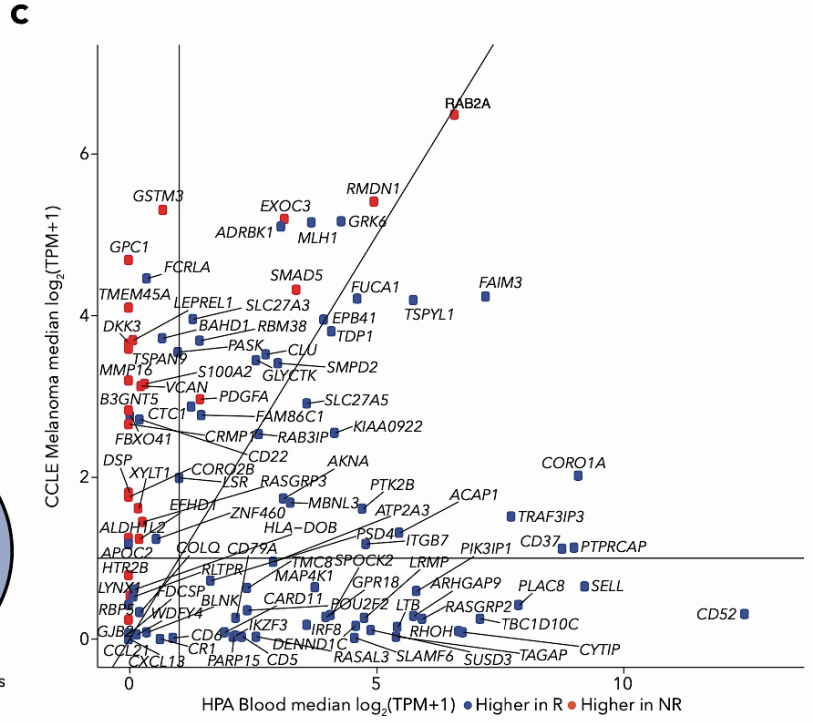
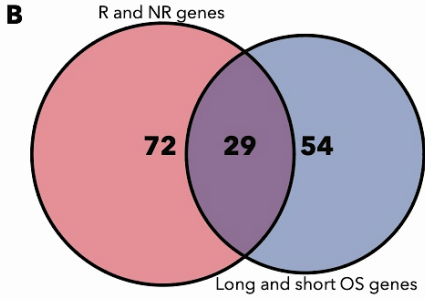
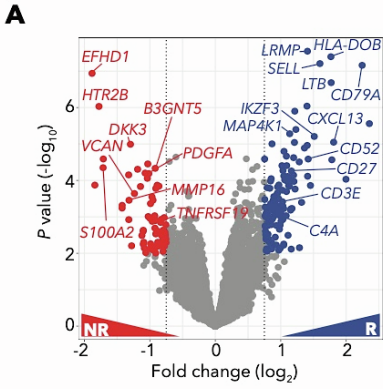
*Tsoi et al (Cancer Cell, 2018)



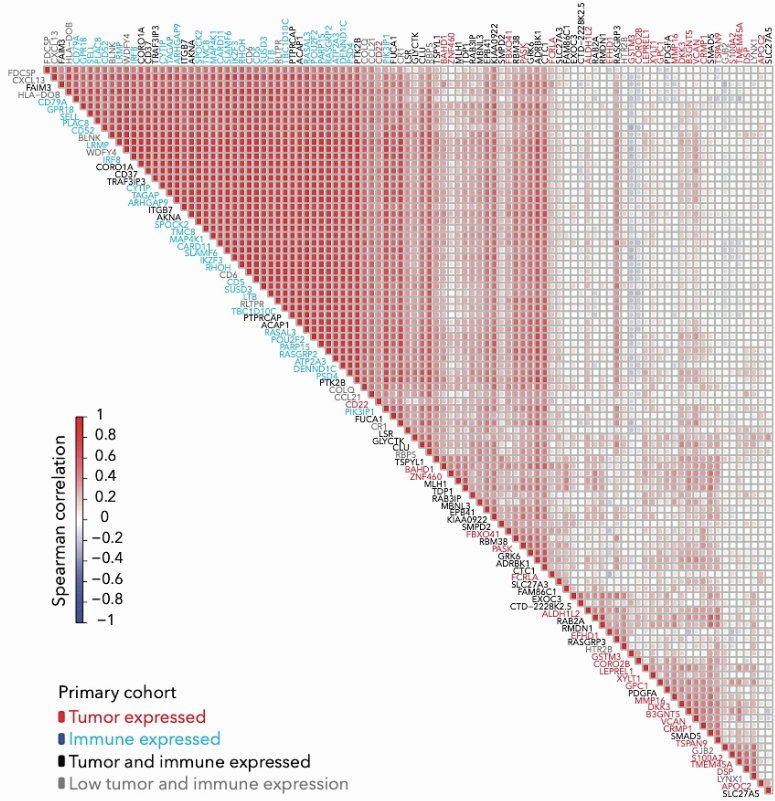
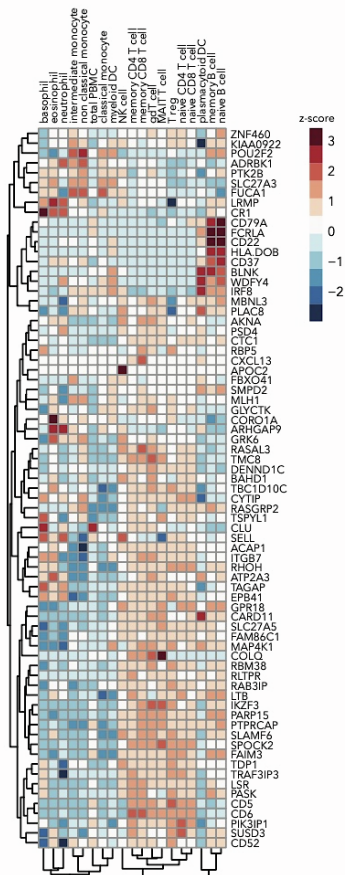
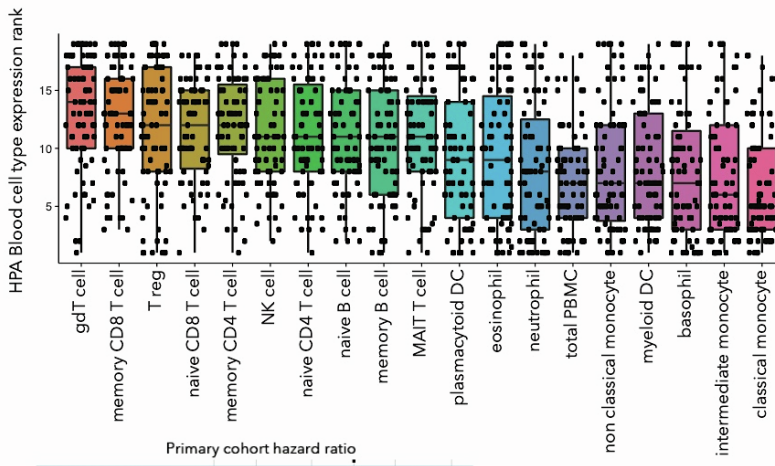
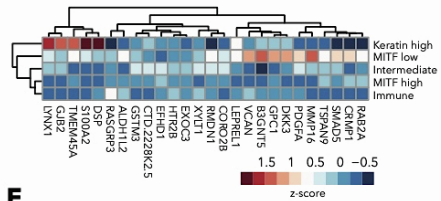
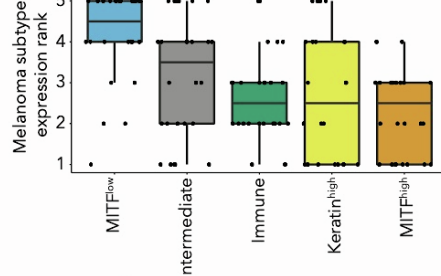
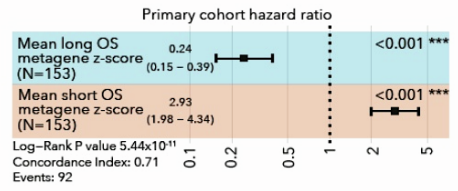
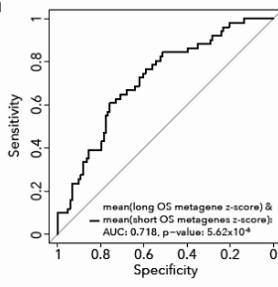
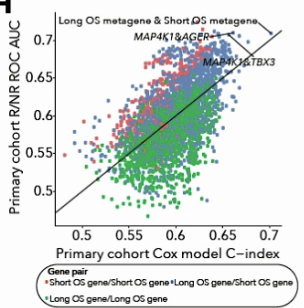
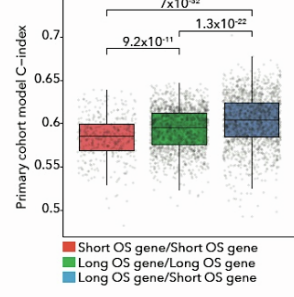
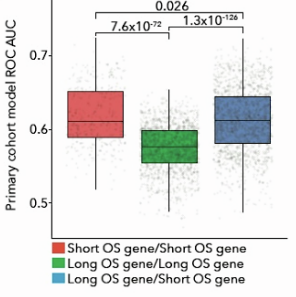
Supplementary Figure 10. Subtypes identified using NMF clustering of TCGA melanoma RNA-seq and their tumor related features, Related to Figure 3. **A.** NMF H matrix from TCGA melanoma NMF clustering (n=469) identified 5 subtypes. Activity values indicate the probability that a sample is associated with a cluster. Samples are sorted by activity value within subtypes. **B.** Comparison of subtype membership to previously identified TCGA subtypes³⁸. **C.** TCGA biopsy locations and subtype membership for all samples. The Immune subtype is enriched for lymph node biopsy samples, but all other subtypes contain lymph node samples as well. **D.** Comparison of subtype membership to melanoma differentiation subtypes⁴⁸. **E.** Boxplots of gene expression for selected TCGA melanoma NMF cluster marker genes. All genes were identified through automated marker selection and were included in the heatmap except *MITF*, *MLANA* and *AXL*. **F.** Heatmap of marker genes identified for each NMF subtype in TCGA melanoma data. Initial $\log_2(\text{TPM}+1)$ values were median centered to obtain $\log_2(\text{Fold change})$ values. We selected marker genes which were overexpressed in each cluster relative to all other samples. **G-J.** Kruskal-wallis p values for association of gene expression with subtype are displayed above plots, **(G)** TMB (\log_{10} scale), **(H)** tumor purity, **(I)** TCB_{RNA} and **(J)** BCB_{RNA} , for TCGA samples by RNA-seq subtype. **K.** Kaplan-Meier survival curve for TCGA samples by RNA-seq subtype.



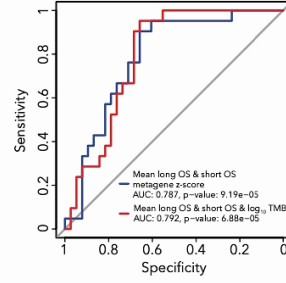
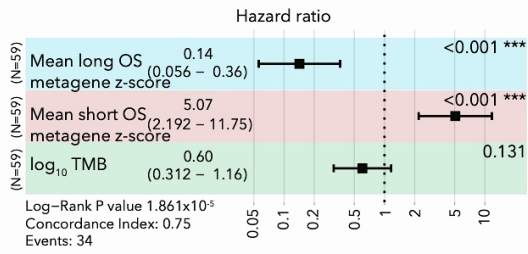
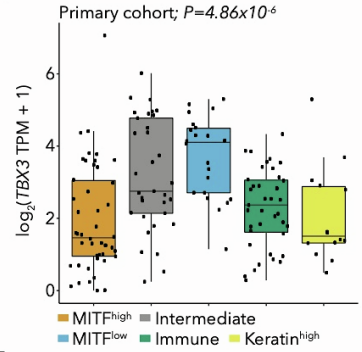
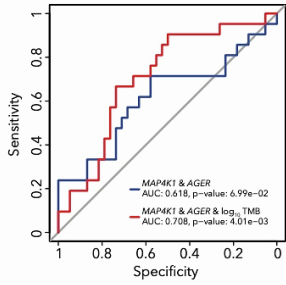
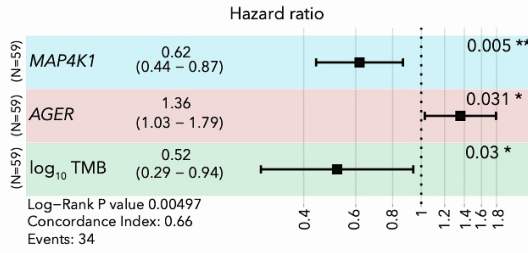
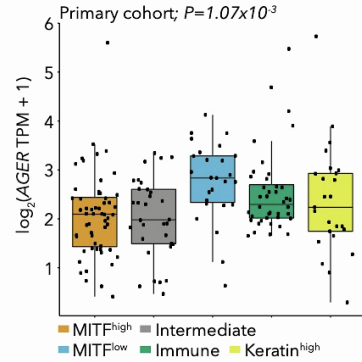
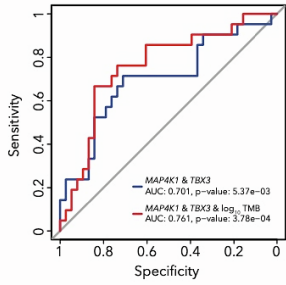
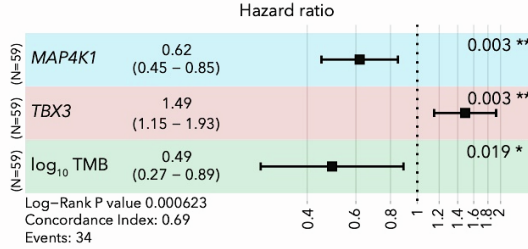
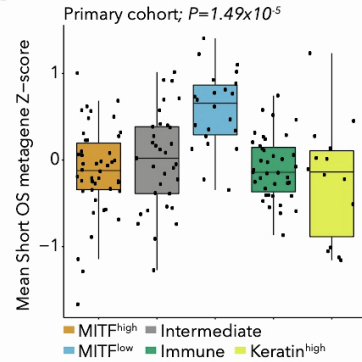
Supplementary Figure 11. Subtype classification for primary cohort RNA-seq samples, Related to Figure 3. **A.** PCA of protein coding gene $\log_2(\text{TPM}+1)$ values before (upper plot) and after batch effects correction with ComBat⁸³ (lower plot). Before batch effects correction, samples cluster by cohort and library preparation method (polyA selection vs. transcriptome capture). **B.** NMF H matrix for primary cohort sample subtyping using subtypes and marker genes identified in TCGA melanoma samples. **C.** Subtypes by RNA-seq sample for each sample in the primary cohort. **D-G.** Kruskal-wallis p values for association of gene expression with subtype are displayed above plots, **(D)** TMB (\log_{10} scale), **(E)** tumor purity for RNA-seq samples with matched WES data, **(F)** TCB_{RNA} and **(G)** BCB_{RNA} . **H.** Number of responders and non-responders by subtype.



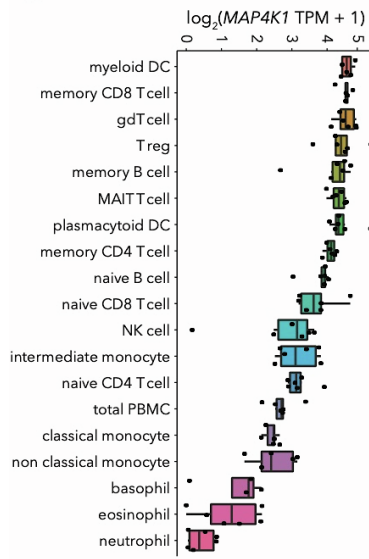
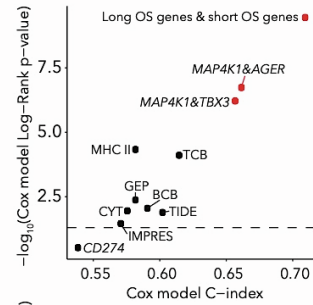
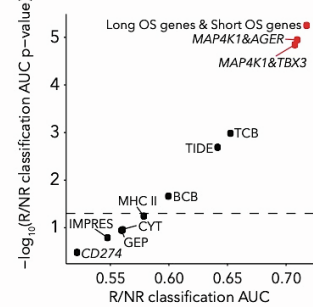
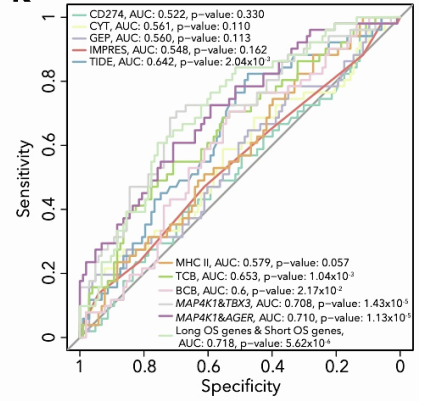
Supplementary Figure 12. Genes associated with response in the primary cohort and expression patterns for long and short OS differentially expressed genes in the primary cohort, Related to Figure 3. **A.** Differential expression between responders (R) and non-responders (NR) in the primary cohort. **B.** Venn diagram for differentially expressed genes in the high vs. low OS and responder vs. non-responder comparisons. In total, 29 genes were differentially expressed in both analyses. **C.** Expression of responder and non-responder differentially expressed genes in melanoma CCLE cell lines and Human Protein Atlas blood cell types. **D.** Co-expression for long and short OS differentially expressed genes in the primary cohort. **E.** Expression of genes overexpressed in long OS patients in Human Protein Atlas (HPA) blood cell types. **F.** Ranks of HPA cell type expression for genes overexpressed in long OS patients. **G.** Expression of genes overexpressed in short OS patients in primary cohort samples grouped by melanoma subtype. **H.** Ranks of melanoma subtype expression for genes overexpressed in short OS patients.

A**B****C****D****E****F****G****H****I****J**

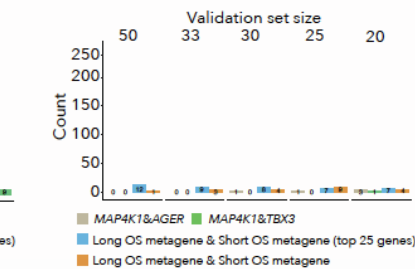
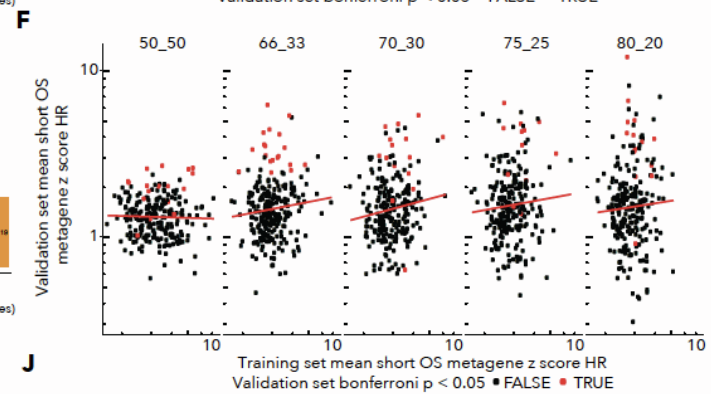
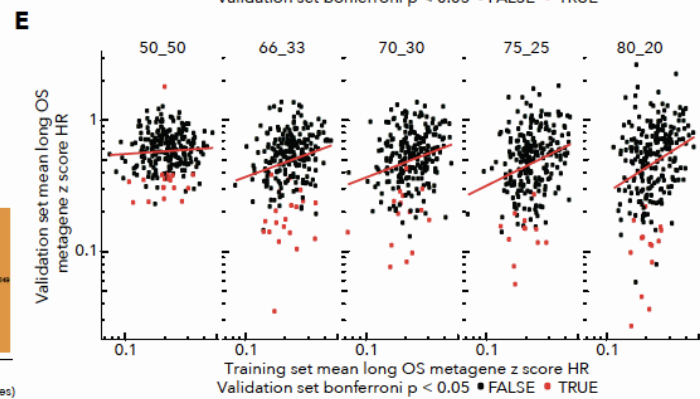
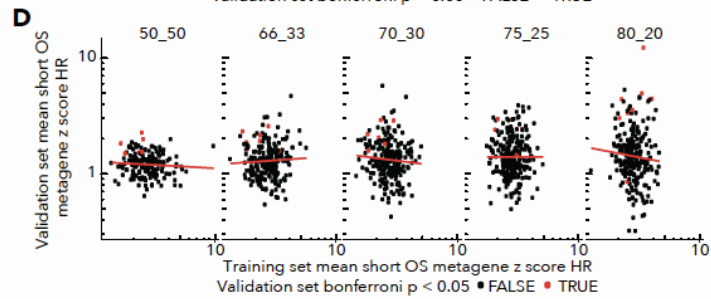
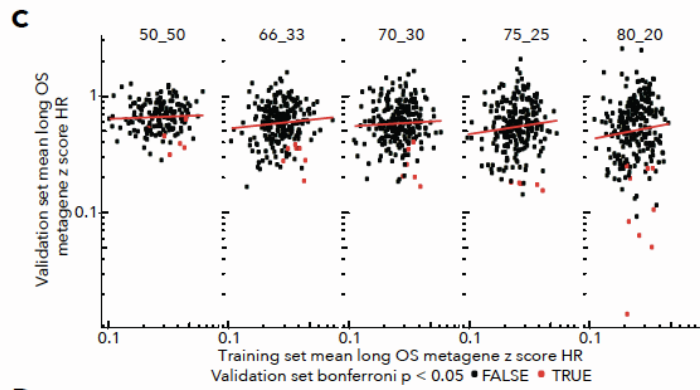
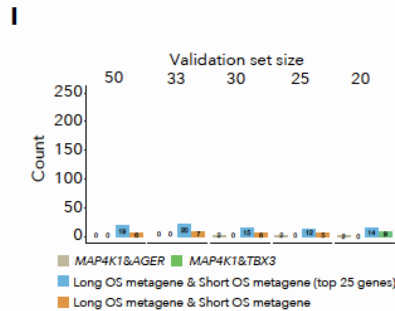
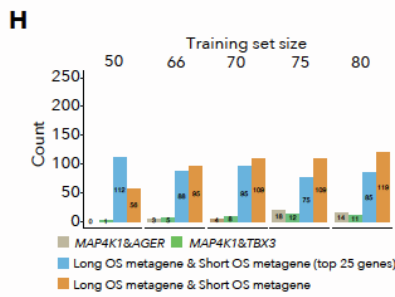
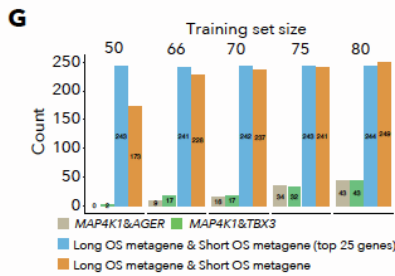
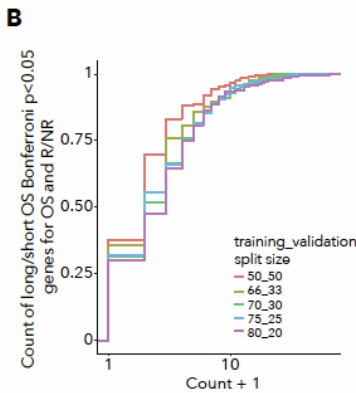
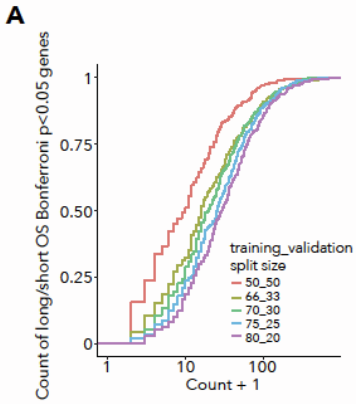
Supplementary Figure 13. Expression patterns for responder and non-responder differentially expressed genes and performance of gene-pair models in the primary cohort in the primary cohort, Related to Figure 3 and Figure 4. **A.** Co-expression for responder and non-responder differentially expressed genes in the primary cohort. **B.** Expression of genes overexpressed in responders in Human Protein Atlas (HPA) blood cell types. **C.** Ranks of HPA cell type expression for genes overexpressed in responders. **D.** Expression of genes overexpressed in non-responders in primary cohort samples grouped by melanoma subtype. **E.** Ranks of melanoma subtype expression for genes overexpressed in non-responders. **F.** Forest plot for the long OS and short OS metagene pair model in the primary cohort. Error bars represent 95% confidence intervals for Cox model hazard ratio estimates. **G.** ROC curve for the long OS and short OS metagene pair model in the primary cohort. **H.** Performance for all gene pair models using genes derived from long OS vs. short OS differential expression in terms of survival and response predictions in the primary cohort based on survival C-index and response AUC. Each point represents one gene pair model, and points are colored by the gene pair type (Short OS/Short OS gene pair- red, Long OS/Long OS gene pair- green or Short OS/Long OS gene pair- blue). **I.** Survival C-index for gene pair models using genes derived from long OS vs. short OS differential expression by gene pair type. **J.** Response AUC for gene pair models using genes derived from long OS vs. short OS differential expression by gene pair type.

A**E****B****F****C****G****D**

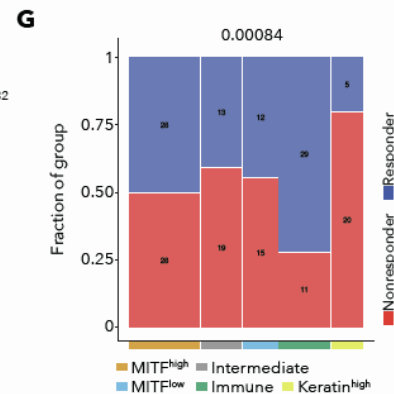
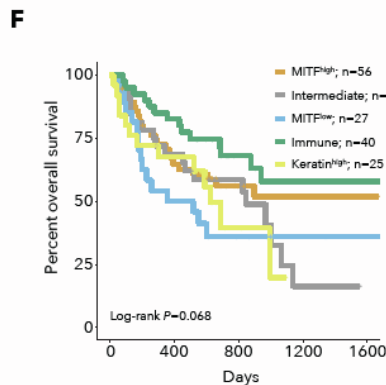
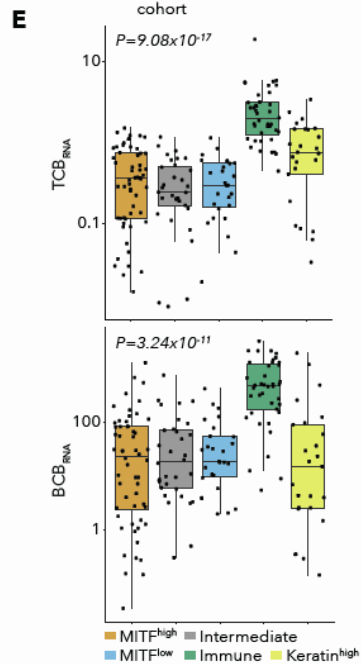
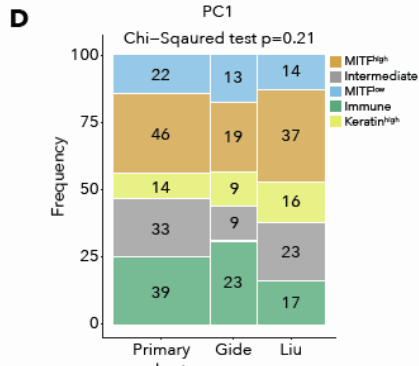
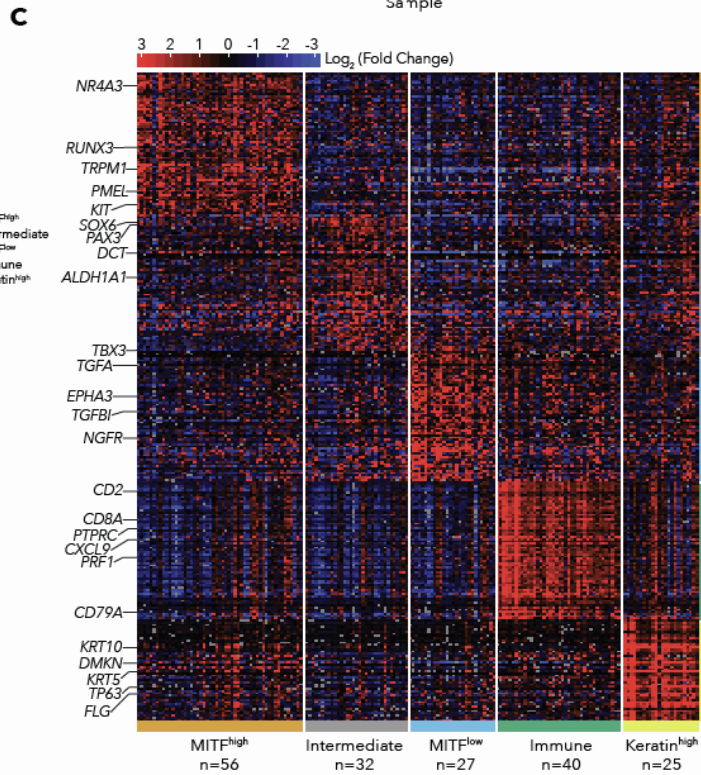
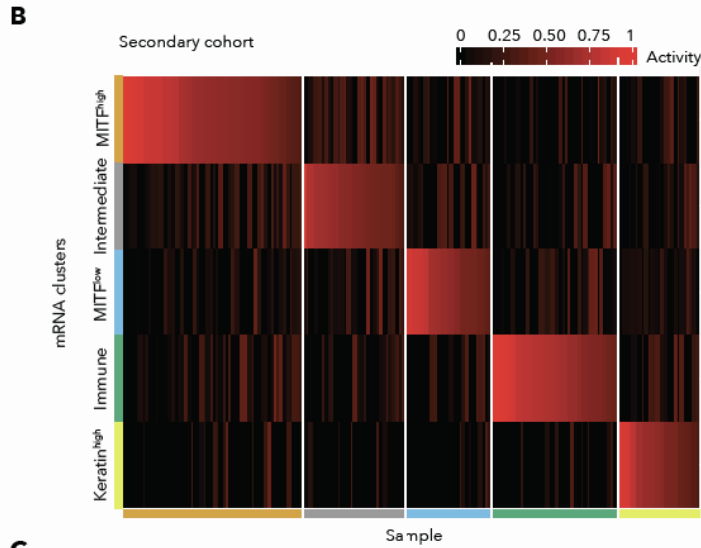
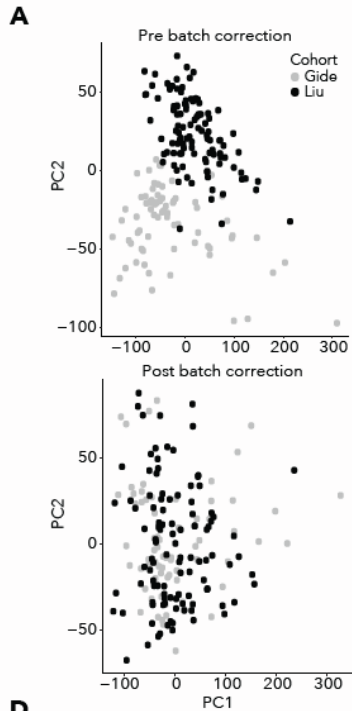
Model	Likelihood Ratio Test p value for OS model with vs. without log ₁₀ (TMB)	DeLong's Test p value for Response model with vs. without log ₁₀ (TMB)
MAP4K1 & AGER	0.0304	0.125
MAP4K1 & TBX3	0.0194	0.223
Long OS metagene & Short OS metagene	0.133	0.879

H**I****J****K**

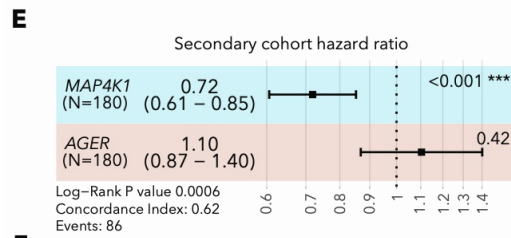
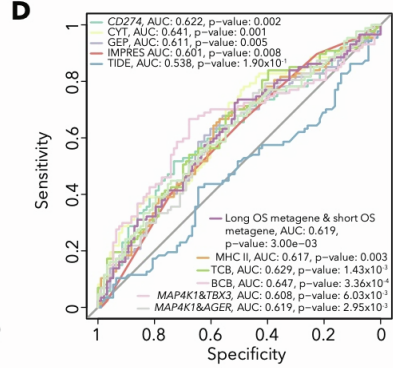
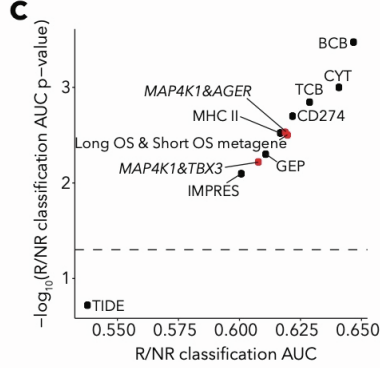
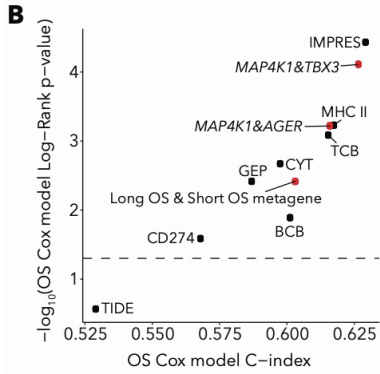
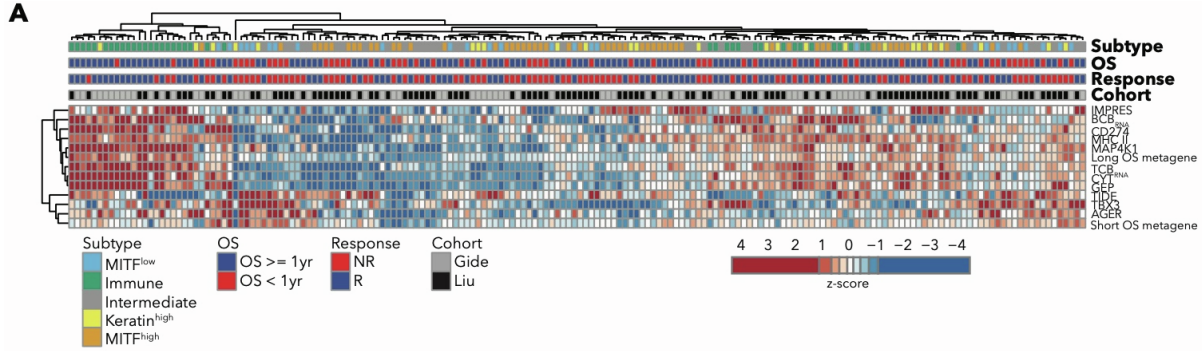
Supplementary Figure 14. Performance of the three RNA gene-pair models with TMB in the primary cohort, expression of genes from top gene pair models and gene pair model performance, Related to Figure 4. **A.** Forest plot (upper) for Cox survival model and ROC curves for response classification (lower) incorporating long OS metagene, short OS metagene and TMB in the primary cohort. Error bars represent 95% confidence intervals for Cox model hazard ratio estimates. **B.** Forest plot (upper) for Cox survival model and ROC curves for response classification (lower) incorporating *MAP4K1* expression, *AGER* expression and TMB in the primary cohort. Error bars represent 95% confidence intervals for Cox model hazard ratio estimates. **C.** Forest plot (upper) for Cox survival model and ROC curves for response classification (lower) incorporating *MAP4K1* expression, *TBX3* expression and TMB in the primary cohort. Error bars represent 95% confidence intervals for Cox model hazard ratio estimates. **D.** Likelihood ratio test and DeLong's test results comparing Cox survival models or response model ROC curves, respectively for the *MAP4K1&AGER*, *MAP4K1&TBX3* or long OS metagene & short OS metagene pair with or without TMB in the primary cohort. **E.** Expression of *TBX3* in the primary cohort by melanoma subtype with Kruskal-Wallis test P-value. **F.** Expression of *AGER* in the primary cohort by melanoma subtype with Kruskal-Wallis test P-value. **G.** Expression of the short OS metagene in the primary cohort by melanoma subtype with Kruskal-Wallis test P-value. **H.** Expression of *MAP4K1* in Human Protein Atlas (HPA) cell types. **I.** Performance of melanoma immunotherapy survival models in the primary cohort in terms of C-index and Cox model log-rank P-value. **J.** Performance of melanoma immunotherapy response models in the primary cohort in terms of AUC and AUC P-value. **K.** ROC curves for response classification for all models in the primary cohort.



Supplementary Figure 15. Cross-validation of gene pair model discovery and validation in the primary cohort, Related to Figure 4. **A.** Empirical cumulative distribution of the number of gene pairs discovered with Bonferroni $p < 0.05$ for association with survival in training sets in the cross validation using genes differentially expressed between patients with long and short OS (DESeq $q < 0.05$) within the training set. Each line represents a different training and validation set split size, with 250 cross validation training/validation splits per split size. **B.** Empirical cumulative distribution of the number of gene pairs discovered with Bonferroni $p < 0.05$ for association with survival and response in training sets in the cross validation using genes differentially expressed between patients with long and short OS (DESeq $q < 0.05$) within the training set. Each line represents a different training and validation set split size, with 250 cross validation training/validation splits per split size. **C-D.** Performance of the long OS metagene & short OS metagene model in cross-validation training and validation sets. Each point represents the hazard ratio (HR) of the long OS metagene (**C**) and short OS metagene (**D**) discovered in that training/test set split. In training/validation splits, the metagenes are composed of the genes that were differentially expressed between long and short OS patients with DESeq $q < 0.05$ in the training set samples. Panels represent different split sizes and red lines are linear regressions. Points are colored by whether the metagene had Bonferroni $p < 0.05$ for survival association in the validation set. **E-F.** Performance of the the long OS metagene & short OS metagene model in cross-validation training and validation sets where metagenes were defined using top 25 long OS or short OS genes ranked by DESeq p value. **G-H.** Frequency of selected gene pairs with Bonferroni $p < 0.05$ for association with survival (**G**) or Bonferroni $p < 0.05$ for association with survival and response (**H**) in training sets. Training set sizes are listed above with 250 training/validation splits for each split size. Metagene pair models using the top 25 genes ranked by DESeq p value or the genes with DESeq $q < 0.05$ in the training set are shown separately. **I-J.** Frequency of selected gene pairs with Bonferroni $p < 0.05$ for association with survival (**I**) or Bonferroni $p < 0.05$ for association with survival and response (**J**) in validation sets. Validation set sizes are listed above with 250 training/validation splits for each split size. Metagene pair models using the top 25 genes ranked by DESeq p value or the genes with DESeq $q < 0.05$ in the training set are shown separately.

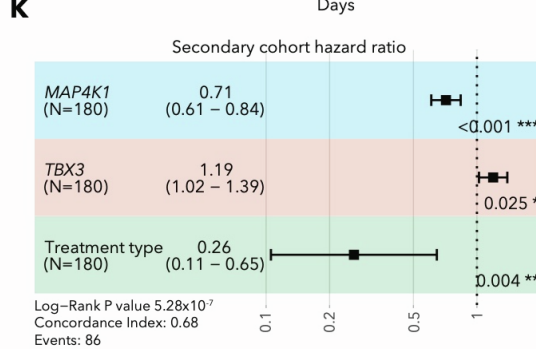
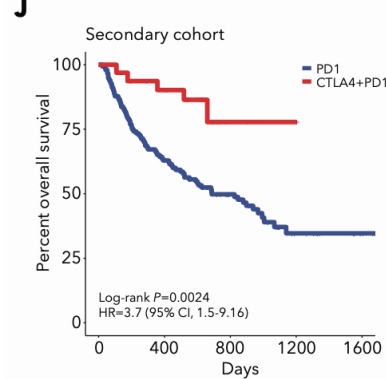
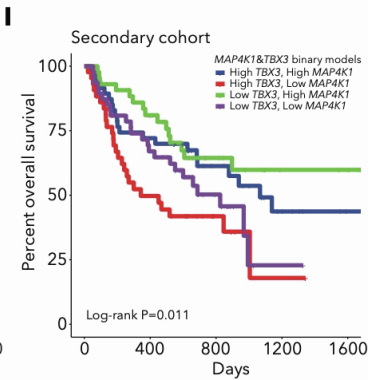
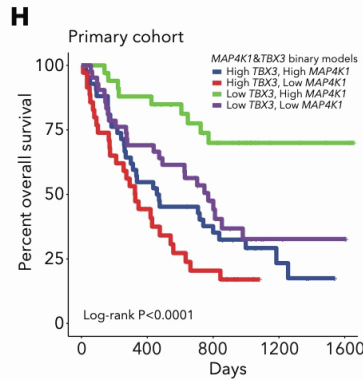
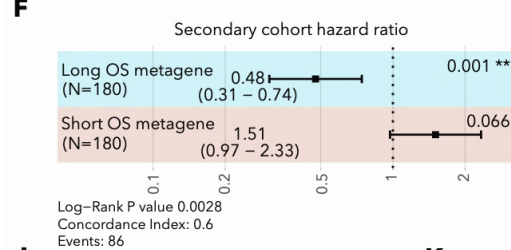


Supplementary Figure 16. Batch effects correction and melanoma subtyping for the secondary cohort, Related to Figure 4. **A.** PCA of secondary cohort (Gide and Liu cohorts) protein coding gene $\log_2(\text{TPM}+1)$ values before (upper plot) and after (lower plot) batch-effects correction with ComBat⁸³. Before batch effects correction, samples cluster by cohort. **B.** NMF H matrix for secondary cohort sample subtyping using subtypes and marker genes identified in TCGA melanoma samples. **C.** Heatmap of marker gene expression for samples in the secondary cohort with samples grouped by subtype. **D.** Comparison of frequency of subtypes in the primary cohort and the Gide and Liu cohorts. **E.** TCB_{RNA} and BCB_{RNA} by subtype for secondary cohort samples with Kruskal-Wallis P values for associations with subtype. **F.** Kaplan-Meier survival curve by subtype for patients in the secondary cohort. **G.** Number of responder and non-responders by subtype in the secondary cohort with Fisher's exact test P value.

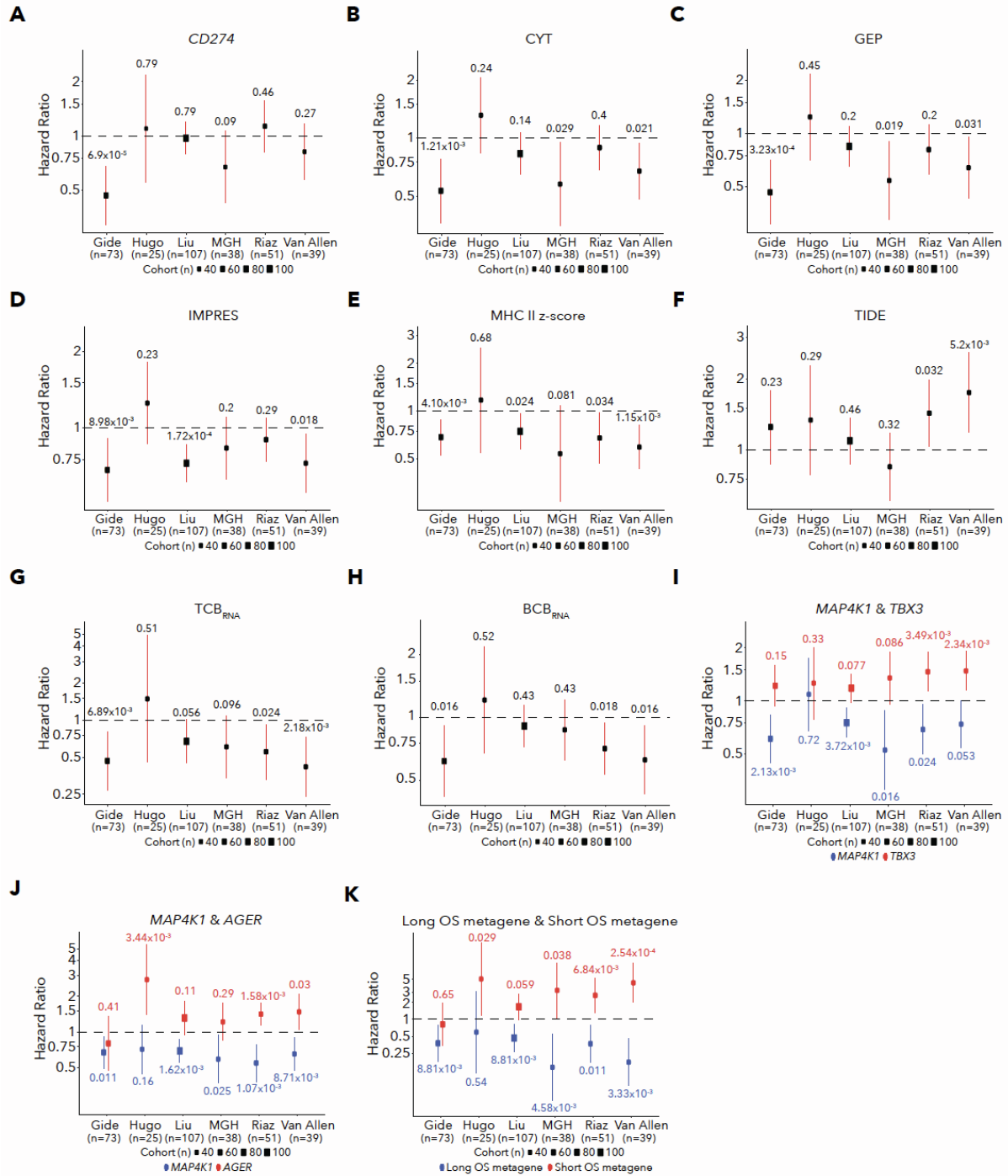


G

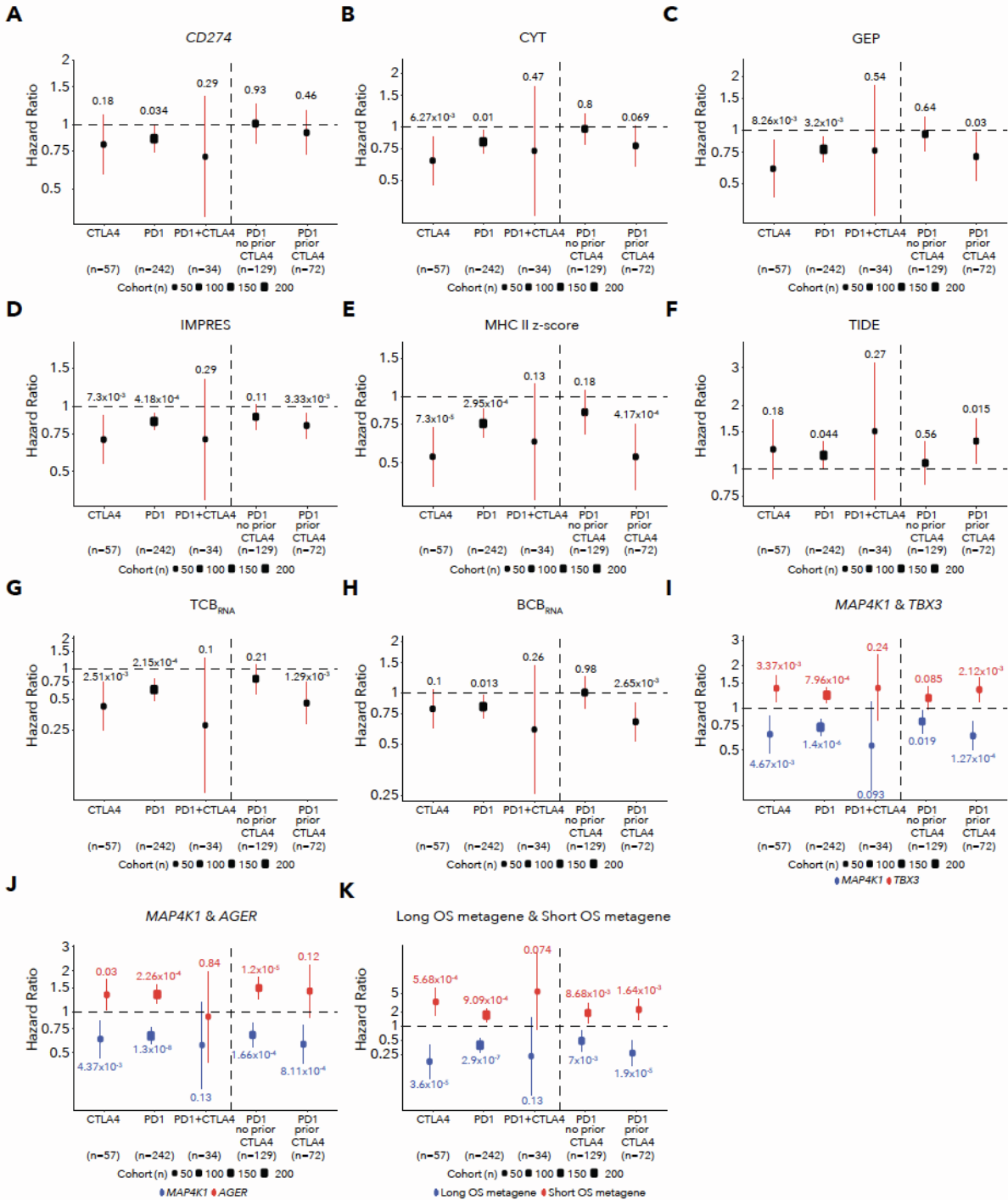
Cohort	Likelihood Ratio Test p for MAP4K1&TBX3 model vs. MAP4K1 model	Likelihood Ratio Test p for MAP4K1&TBX3 model vs. TBX3 model
Primary	4.80x10 ⁻⁵	6.41x10 ⁻⁵
Secondary	2.57x10 ⁻²	3.3x10 ⁻⁵



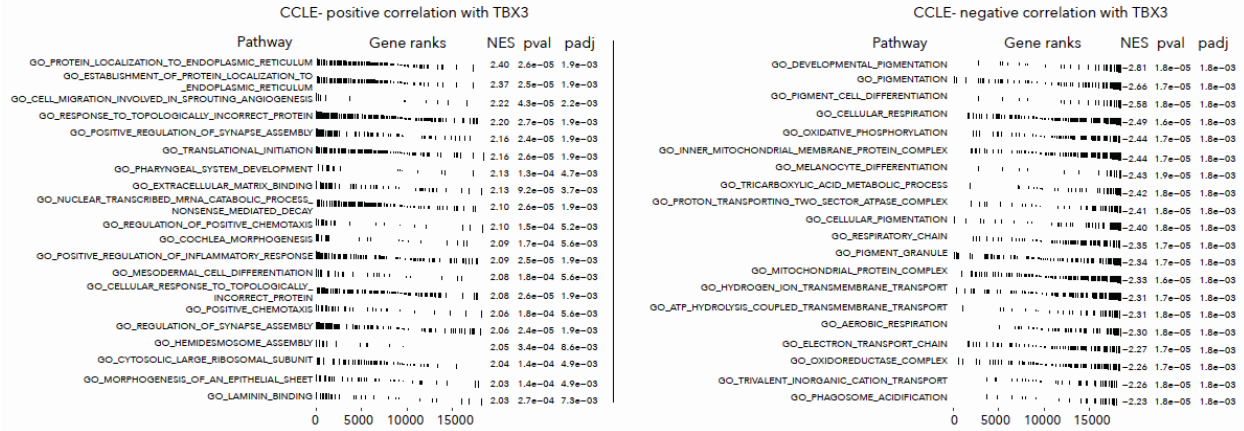
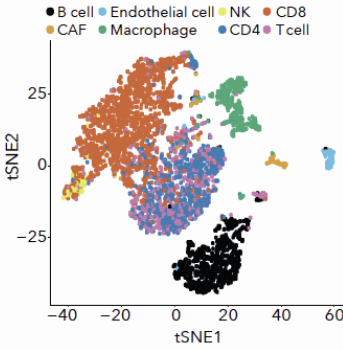
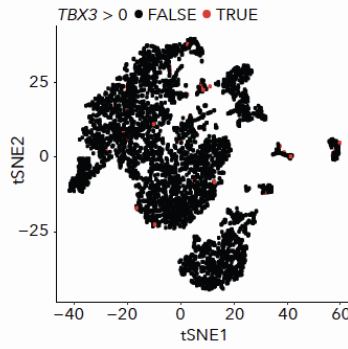
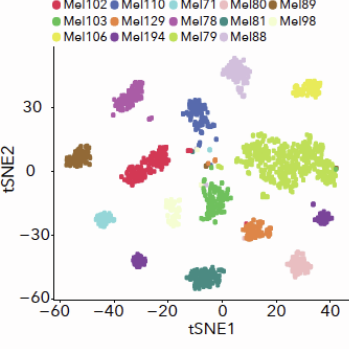
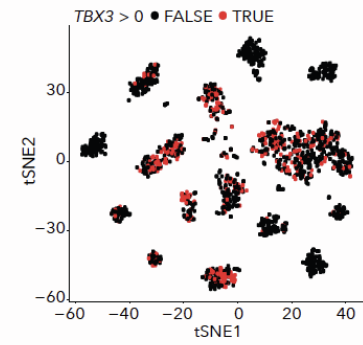
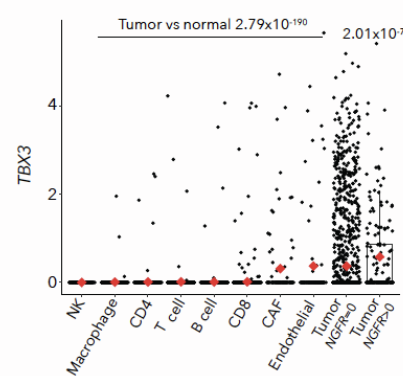
Supplementary Figure 17. Performance of top gene pair models in the secondary cohort, Related to Figure 4. **A.** Heatmap of z-scored values for immunotherapy predictive models and top gene pairs in the secondary cohort. **B.** Performance of pairwise gene models in comparison to previous immunotherapy predictive models in significance and effect size of predictions of survival in the secondary cohort. **C.** Performance of pairwise gene models in comparison to previous immunotherapy predictive models in significance and effect size of predictions of response in the secondary cohort. **D.** ROC curve of pairwise gene models and previous immunotherapy models in classification of response in the secondary cohort. **E.** Forest plot for *MAP4K1&AGER* gene pair Cox survival model in the secondary cohort. Error bars represent 95% confidence intervals for Cox model hazard ratio estimates. **F.** Forest plot for the metagene pair Cox survival model in the secondary cohort. Error bars represent 95% confidence intervals for Cox model hazard ratio estimates. **G.** Likelihood ratio test results comparing Cox survival models with *MAP4K1&TBX3* to Cox survival models with *MAP4K1* or *TBX3* alone in the primary and secondary cohorts. In both cohorts, the gene pair models outperformed both single gene models. **H.** Kaplan-Meier survival curve for groups based on binary *MAP4K1* and *TBX3* expression (above or below median) in the primary cohort. **I.** Kaplan-Meier survival curve for groups based on binary *MAP4K1* and *TBX3* expression (above or below median) in the secondary cohort. **J.** Kaplan-Meier survival curve for groups based on treatment (PD-1 alone or combination CTLA-4/PD-1 therapy) in the secondary cohort. **K.** Forest plot for Cox survival model incorporating *MAP4K1* expression, *TBX3* expression and treatment (PD-1 alone or combination CTLA-4/PD-1) in the secondary cohort. After including treatment in the model, *MAP4K1* and *TBX3* expression both remain significant. Error bars represent 95% confidence intervals for Cox model hazard ratio estimates.



Supplementary Figure 18. Performance of all models within each cohort separately, Related to Figure 4. A-G. Performance of univariate Cox models within each cohort separately. Hazard ratios and error bars representing 95% confidence intervals of Hazard ratio estimates are plotted and Wald test P values are indicated. (A) *CD274* (B) *CYT* (C) *GEP* (D) *IMPRES* (E) *MHC II* (F) *TIDE* (G) *TCB_{RNA}* (H) *BCB_{RNA}*. I-K. Performance of Cox models using gene pairs within each cohort. Hazard ratios and confidence intervals are colored by the gene or metagene and the Wald test P values are indicated. (I) *MAP4K1&TBX3* (J) *MAP4K1&AGER* (K) metagene pair model.



Supplementary Figure 19. Performance of all models in patients treated with different checkpoint blockade therapies, Related to Figure 4. A-G. Performance of univariate Cox models for different checkpoint blockade therapies. Hazard ratios and error bars representing 95% confidence intervals of Hazard ratio estimates are plotted and Wald test P values are indicated. **(A)** *CD274* **(B)** *CYT* **(C)** *GEP* **(D)** *IMPRES* **(E)** *MHC II* **(F)** *TIDE* **(G)** *TCB_{RNA}* **(H)** *BCB_{RNA}*. **I-K.** Performance of Cox models for patients treated with different therapies using gene pairs. Hazard ratios and confidence intervals are colored by the gene or metagene and the Wald test P values are indicated. **(I)** *MAP4K1&TBX3* **(J)** *MAP4K1&AGER* **(K)** metagene pair model.

A**B****C****D****E****F**

Supplementary Figure 20. Analysis of melanoma *TBX3* expression, Related to Figure 4. **A.** GSEA for genes ordered by spearman correlation of gene expression with *TBX3* gene expression in CCLE melanoma cell lines using GO terms. Top GSEA results for genes positively correlated with *TBX3* (left), and top GSEA results for genes negatively correlated with *TBX3* (right). GO terms associated with genes negatively correlated with *TBX3* include pigmentation and melanocyte gene sets. **B-C.** tSNE plot of scRNA data⁵⁹ from immune cells with cells labelled by lineage (**B**) or *TBX3* expression status (**C**). *TBX3* is rarely expressed in any immune cell type. **D-E.** tSNE plot of scRNA data⁵⁹ from melanoma tumor cells with cells labelled by patient (**D**) or *TBX3* expression status (**E**). *TBX3* is expressed in tumor cells from some patients. **F.** *TBX3* expression in scRNA data⁵⁹ by immune cell type or tumor cell type. Melanoma tumor cells are split between cells with no *NGFR* expression or cells with non-zero *NGFR* expression. Mean expression by group is indicated by red dots. P values for Wilcoxon tests of *TBX3* expression in tumor single cells vs. normal single cells and tumor *NGFR*>0 cells vs. tumor *NGFR*=0 cells are indicated above.